

6640-8522

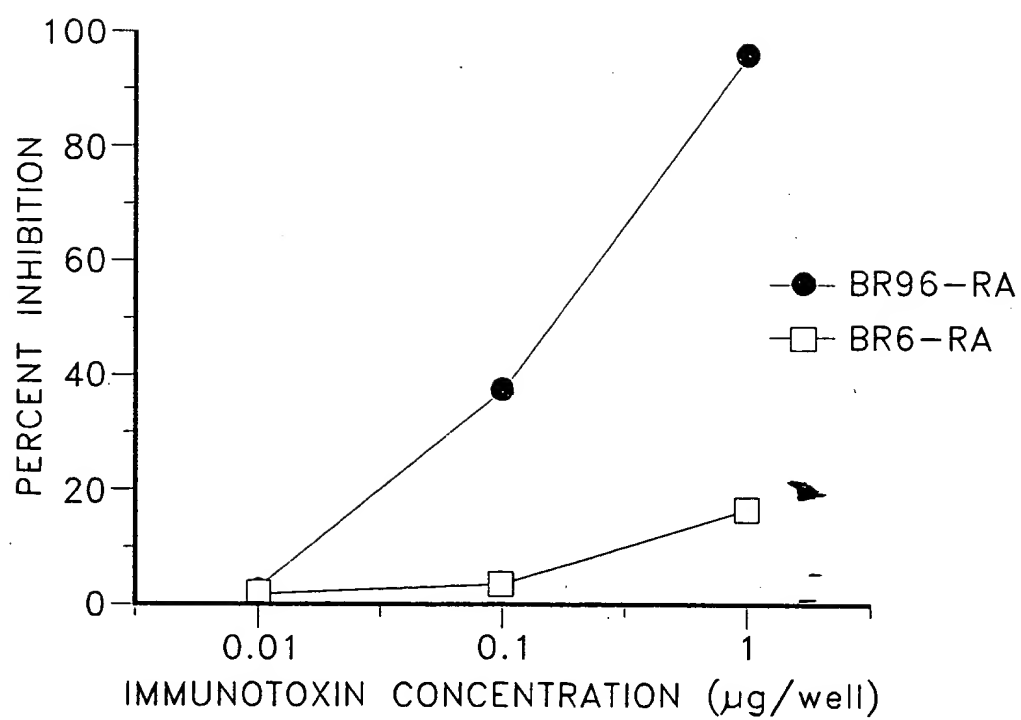


FIG. 1

Immunotoxin Concentration (µg/ml)	BR96-RA (% Inhibition)	BR6-RA (% Inhibition)
0.1	~31	~38
1	~33	~76
10	~75	~98

FIG. 2

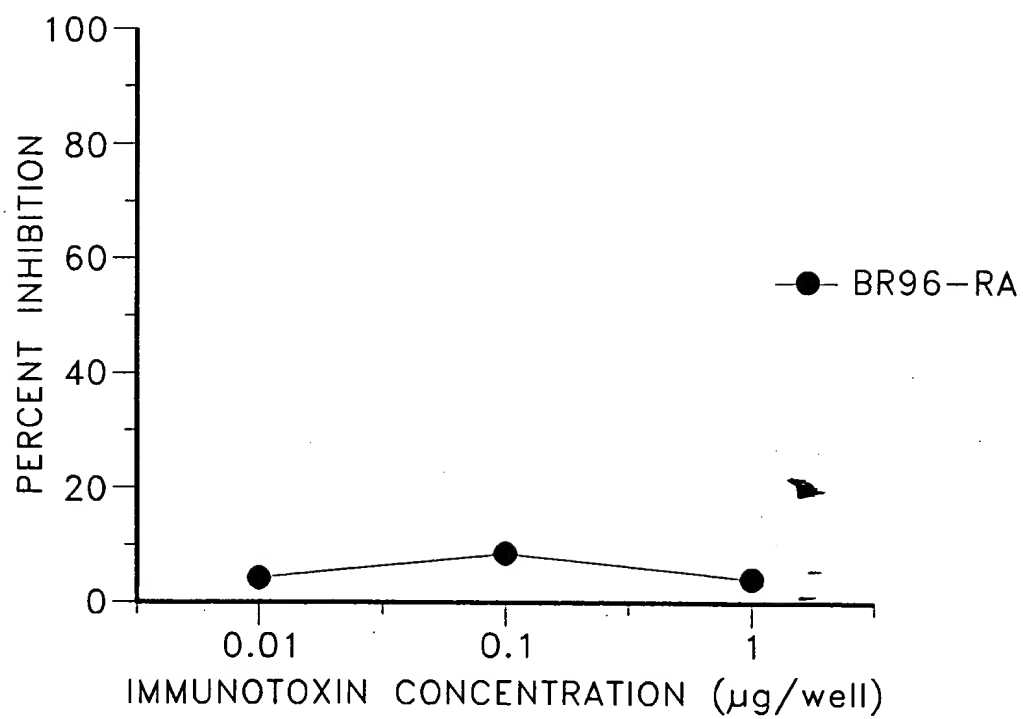


FIG. 3

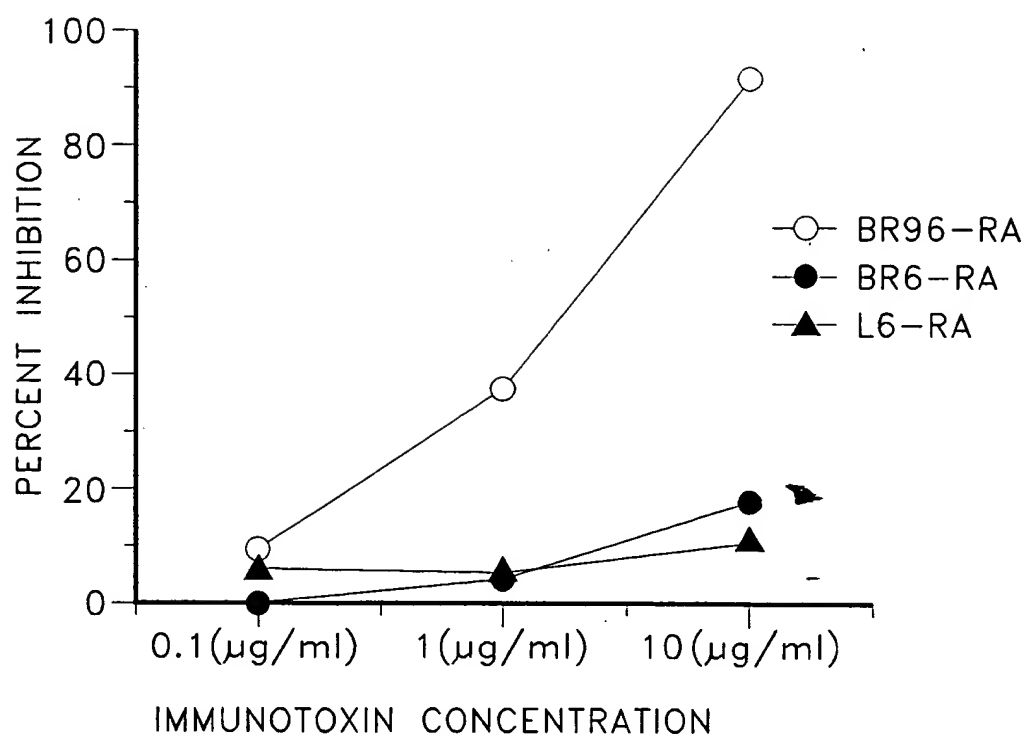


FIG. 4

66443-66443

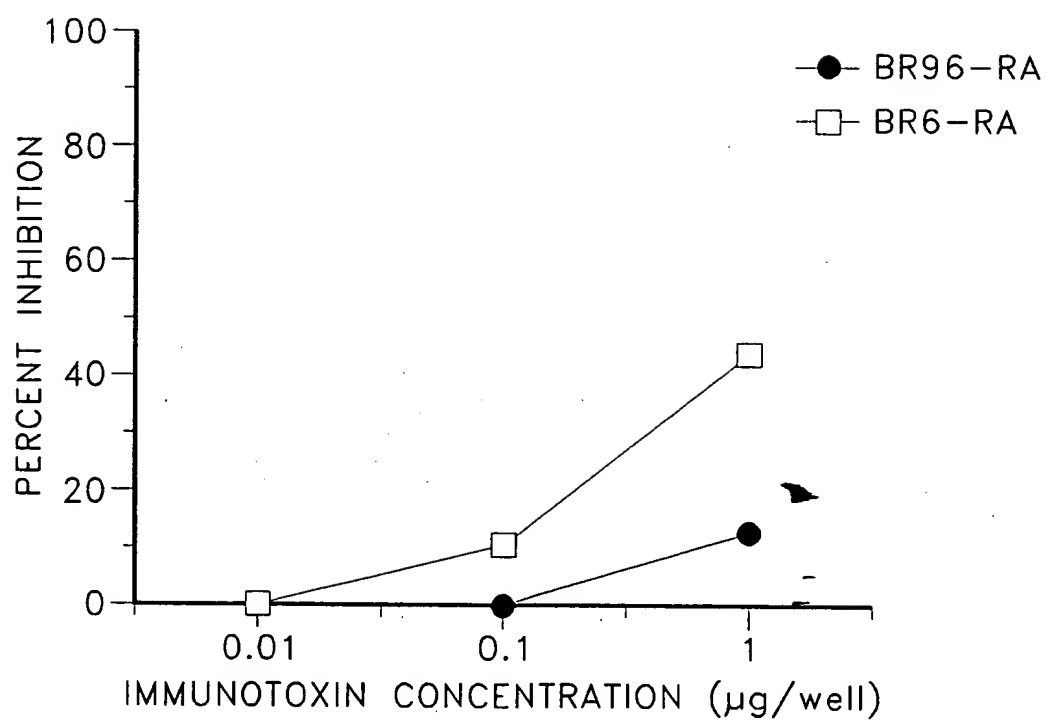


FIG. 5

66649-862666

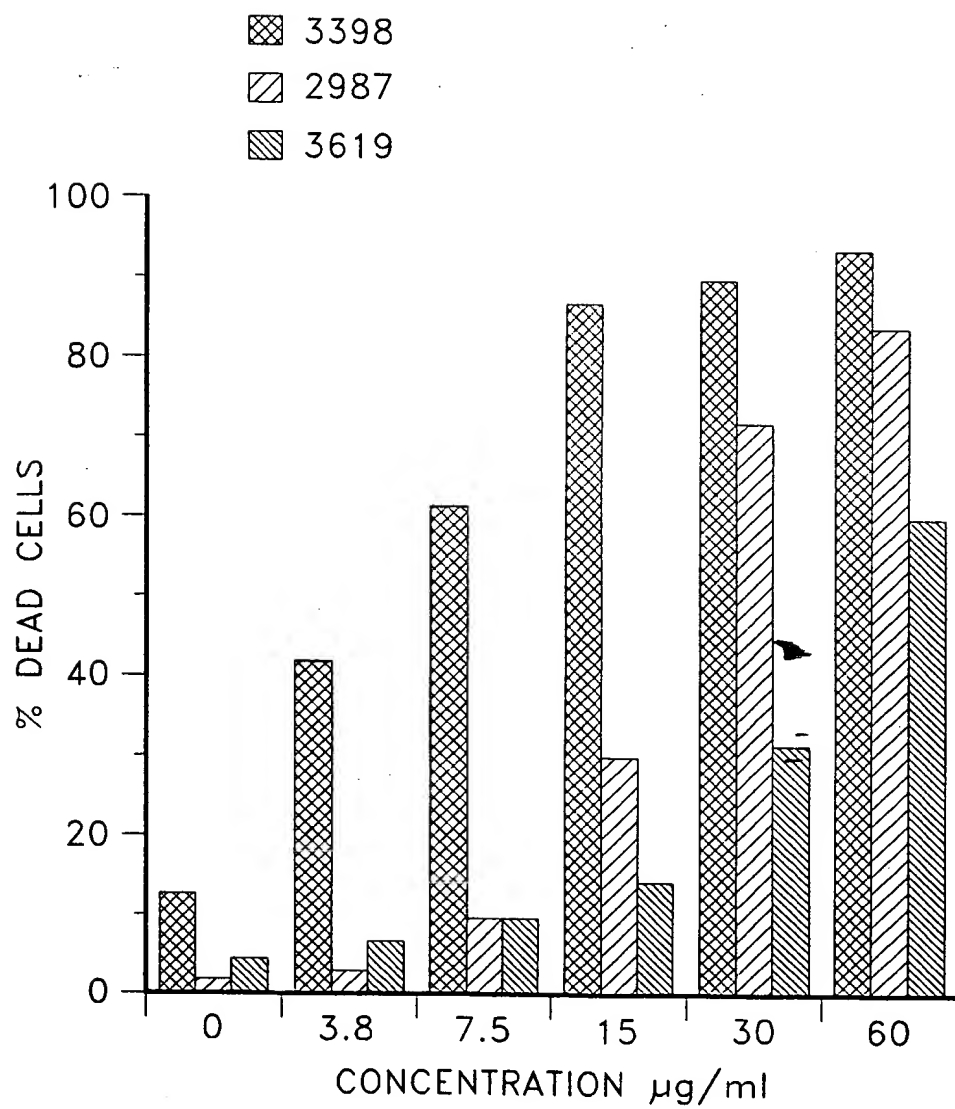


FIG. 6

66640-80000

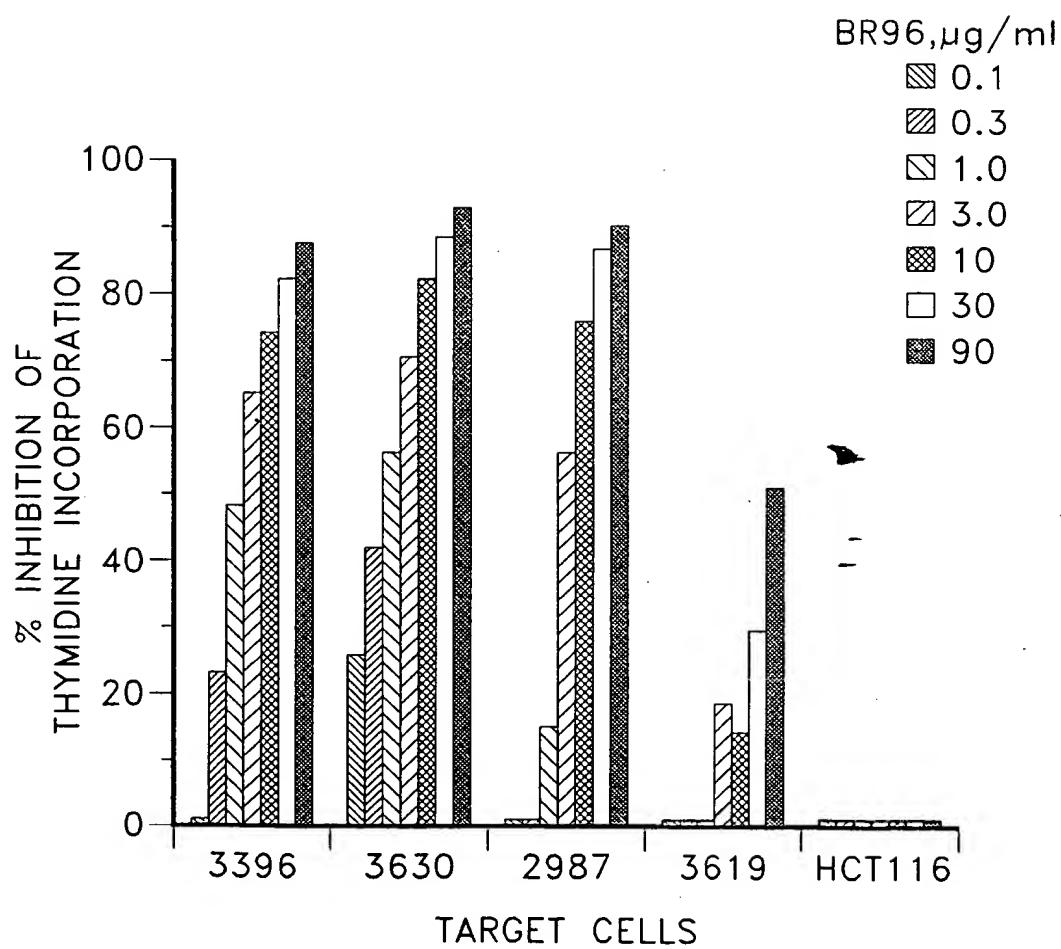


FIG. 7

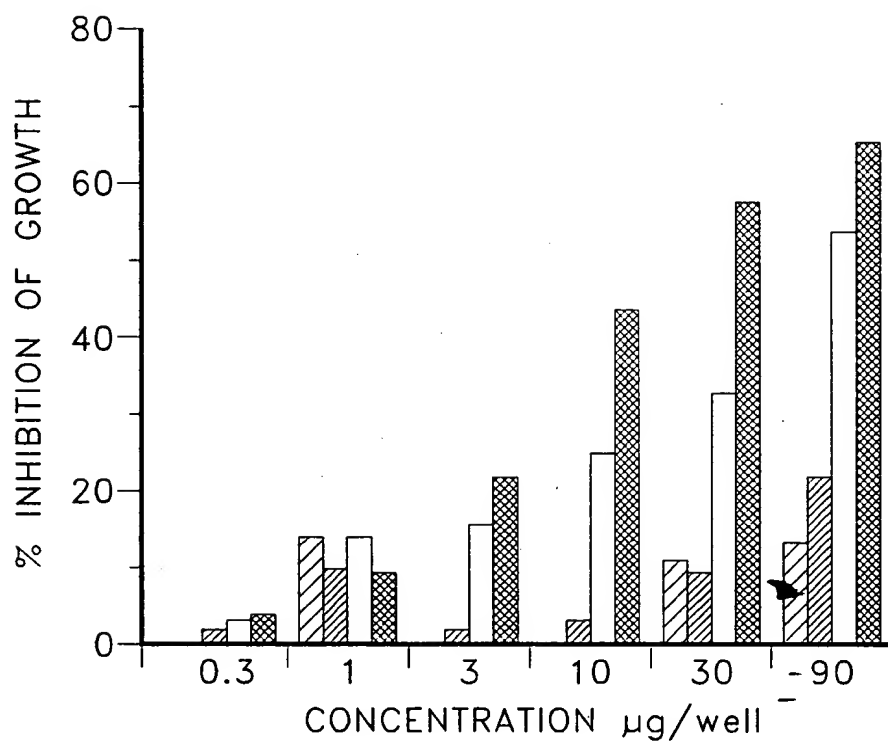


FIG. 8

66640-66660

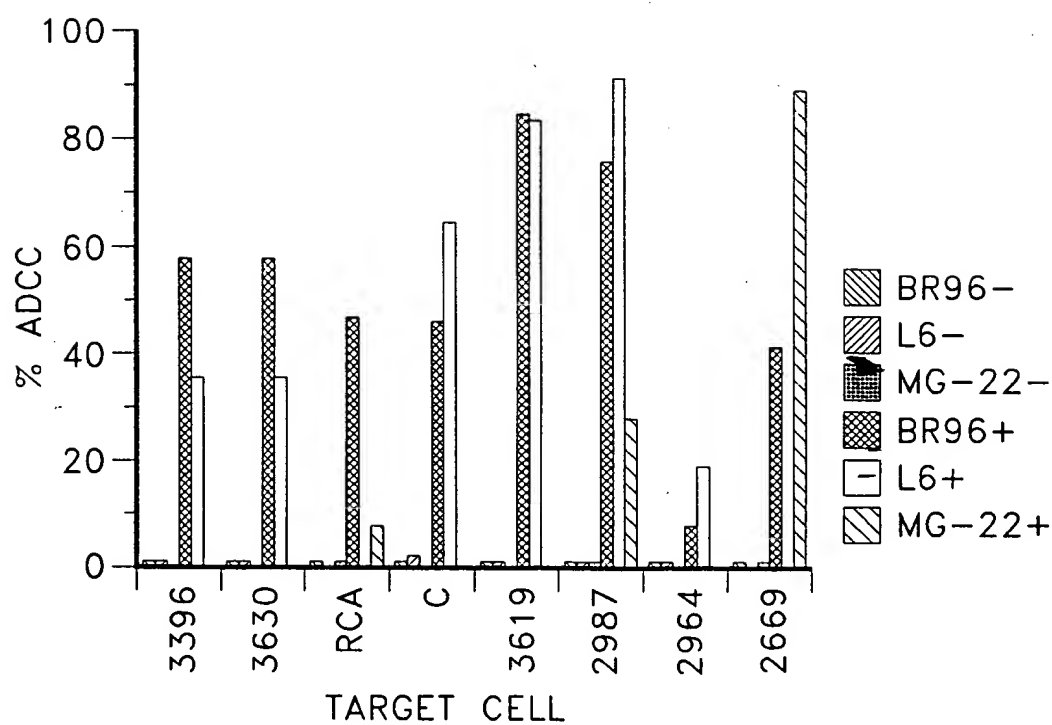


FIG. 9

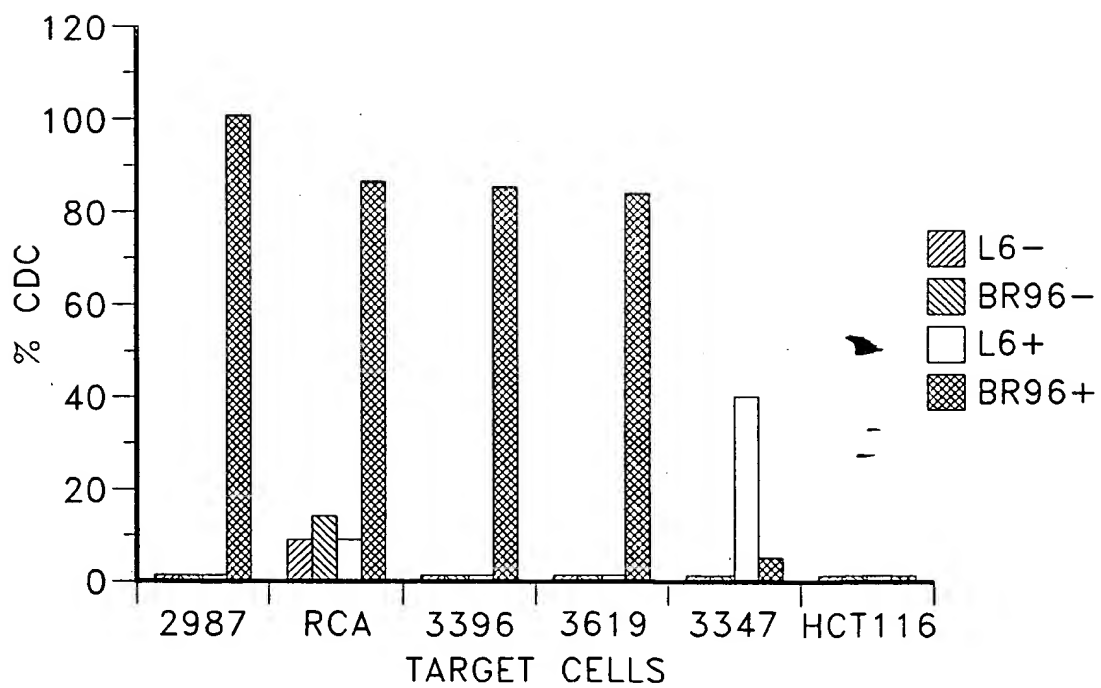


FIG. 10

66443 86205250

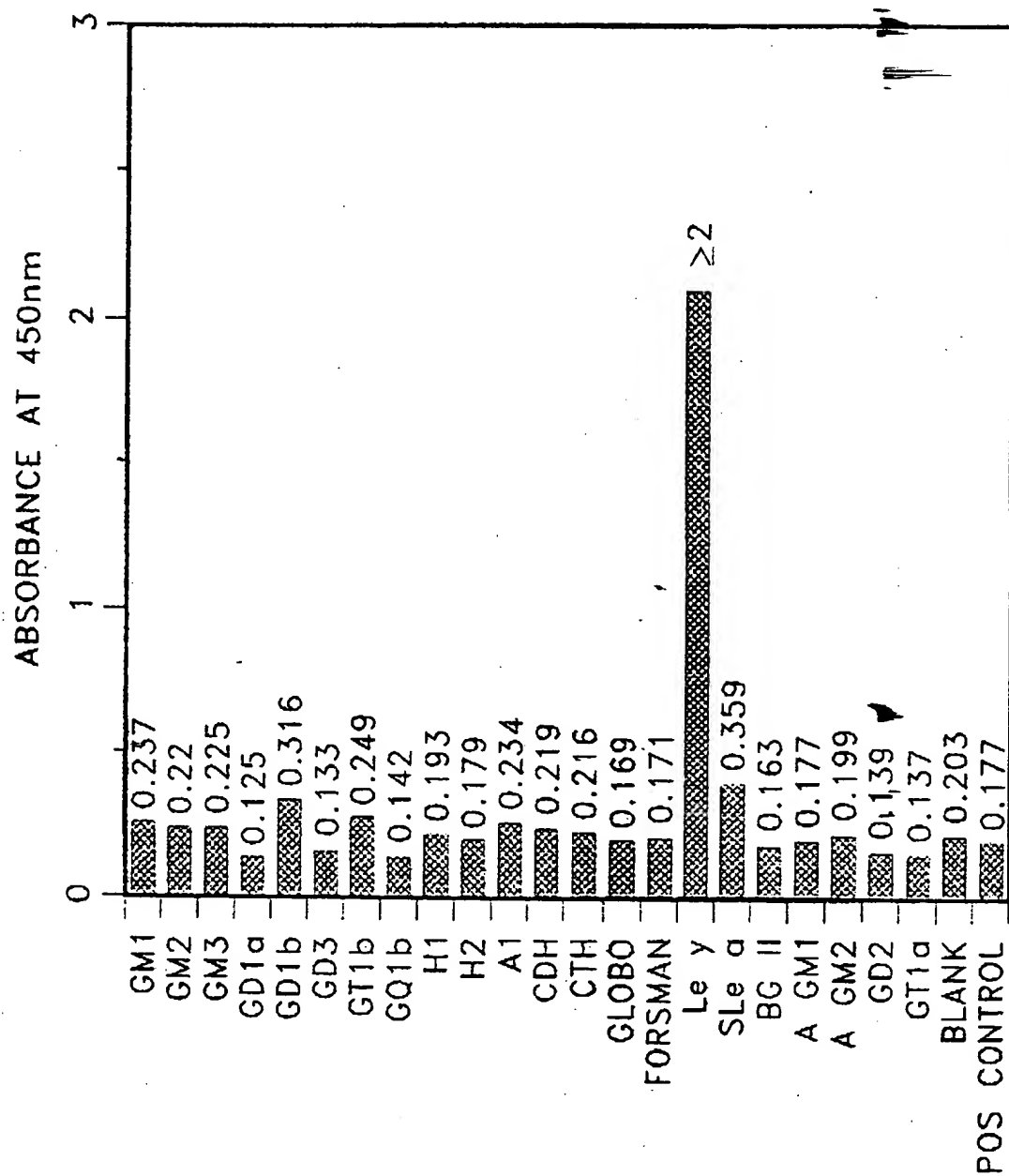


FIG. 11

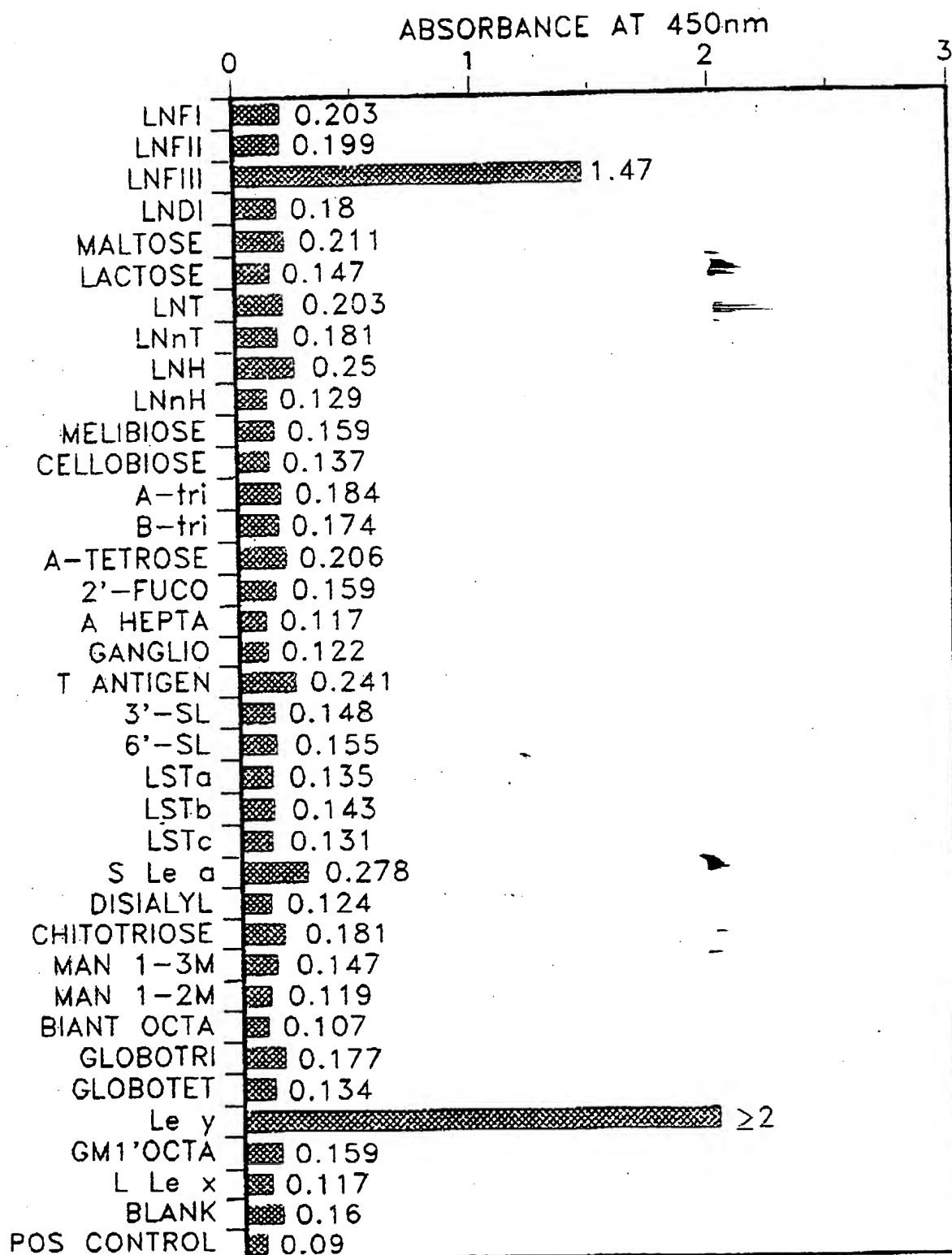


FIG. 12

652740-3626250

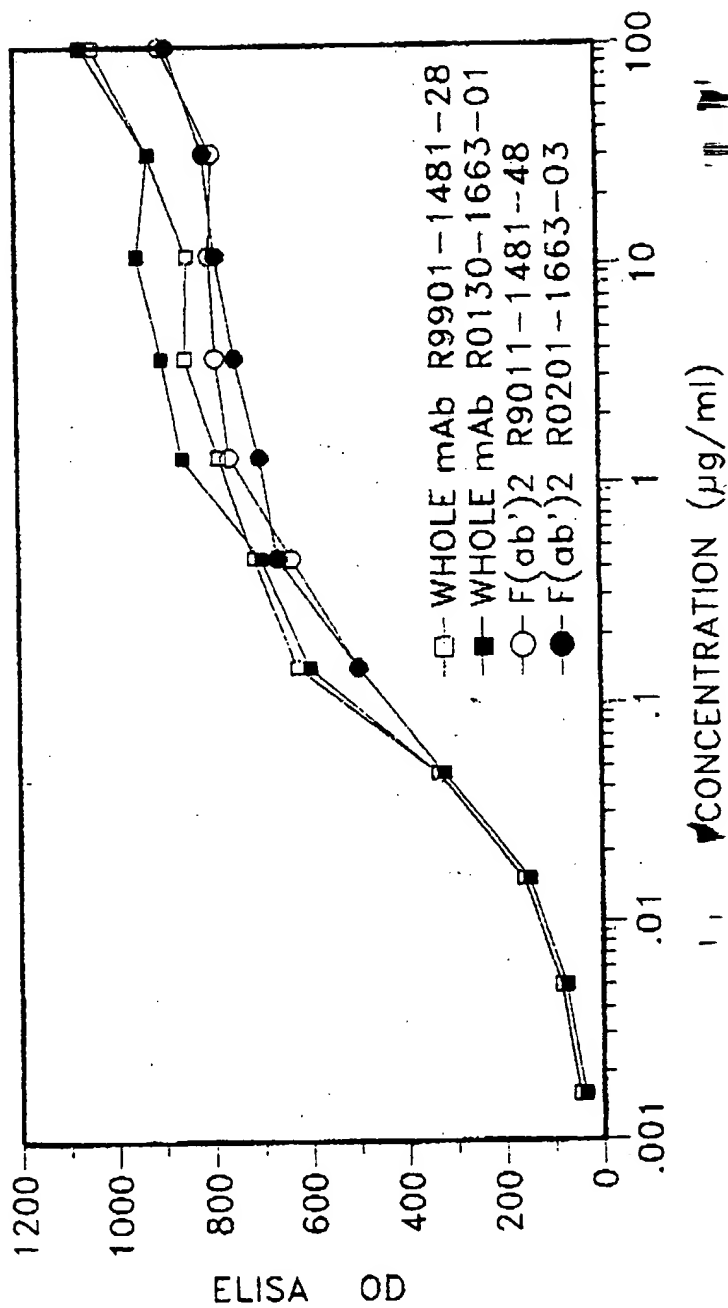


FIG. 13

Figure 1 is a line graph showing the inhibition of anti-CD4 monoclonal antibody binding to CD4⁺ cells by soluble CD4. The Y-axis represents ELISA OD (Optical Density) ranging from 0 to 1200. The X-axis represents CONCENTRATION (µg/ml) on a logarithmic scale ranging from 0.001 to 100. Four curves are plotted, representing different monoclonal antibodies (mAbs) and their corresponding soluble CD4 (sCD4) concentrations:

- R9901-1481-28
- R0130-1663-01
- R9011-1481-48
- R0201-1663-03

The graph shows that the binding of the mAbs to CD4⁺ cells is inhibited by the addition of soluble CD4. The inhibition is most pronounced at higher concentrations of soluble CD4 (10 µg/ml and above), where the OD values for all mAbs drop significantly. The R9901-1481-28 and R0130-1663-01 mAbs show the highest OD values, while the R9011-1481-48 and R0201-1663-03 mAbs show the lowest OD values.

FIG. 14

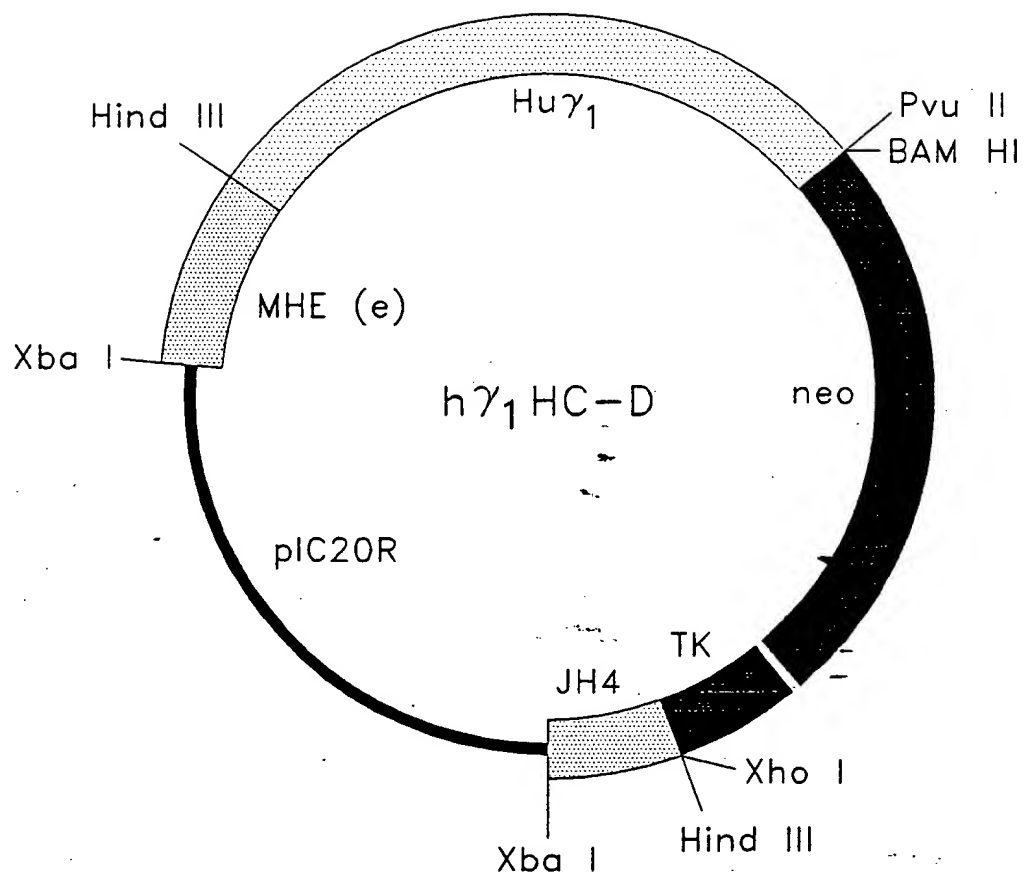


FIG. 15

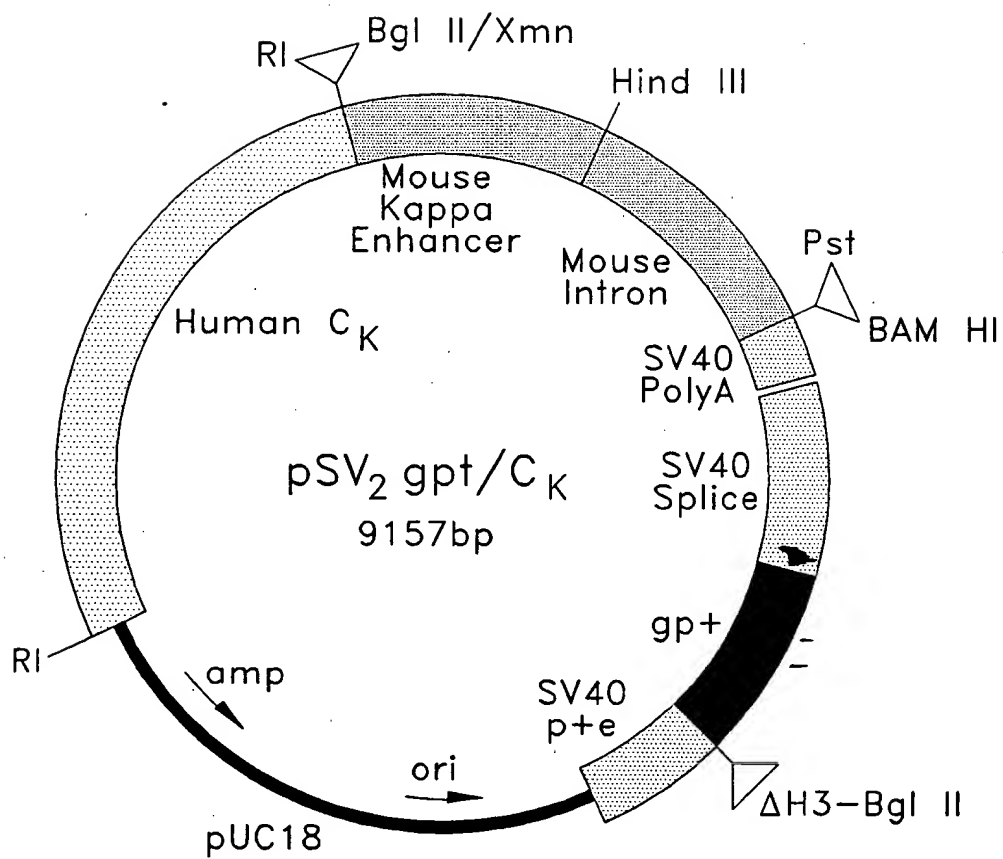


FIG. 16

CHARACTERIZATION OF CHIMERIC ANTIBODY SPECIFICITY AND AFFINITY BY A COMPETITION BINDING ASSAY

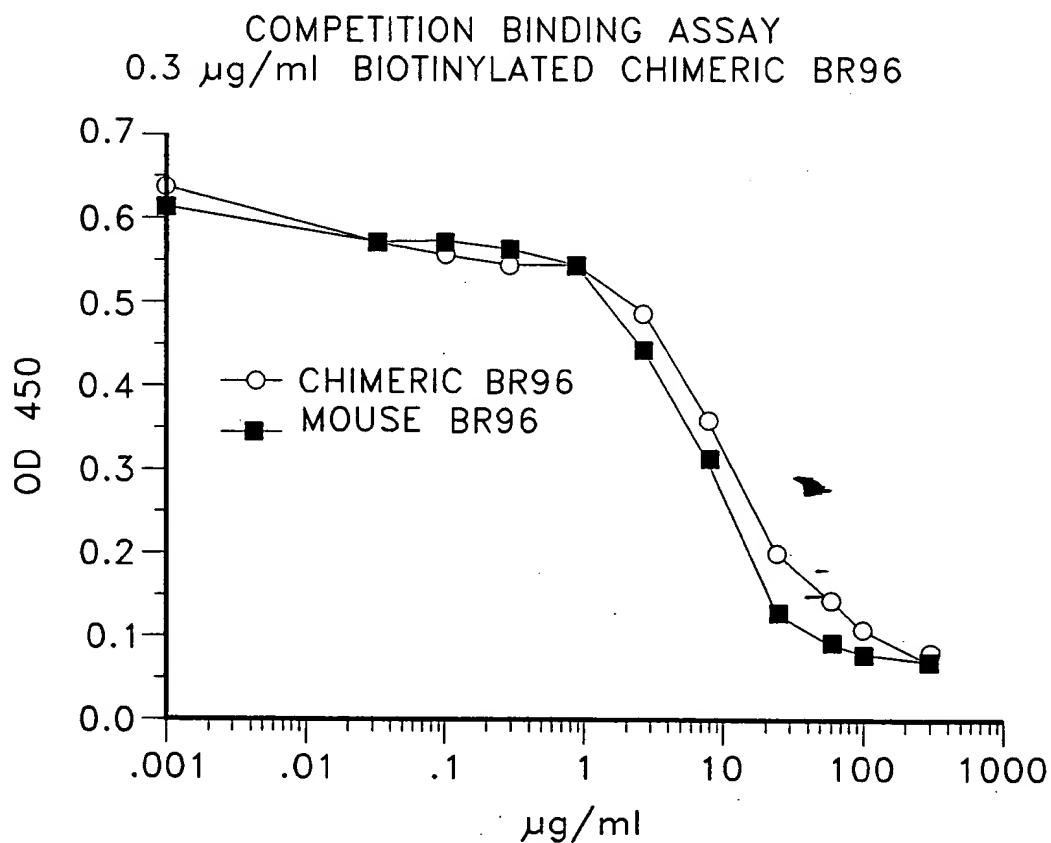


FIG. 17

66E740 36 205363

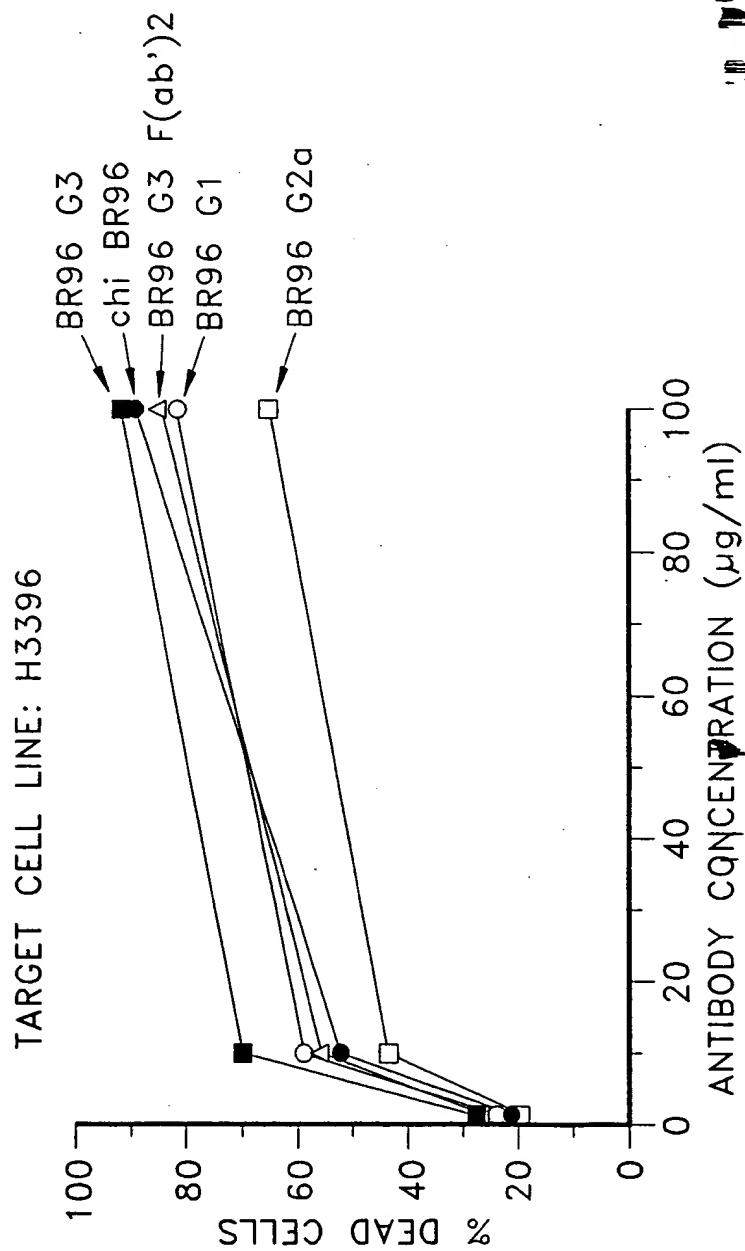


FIG. 18

664740-8620550

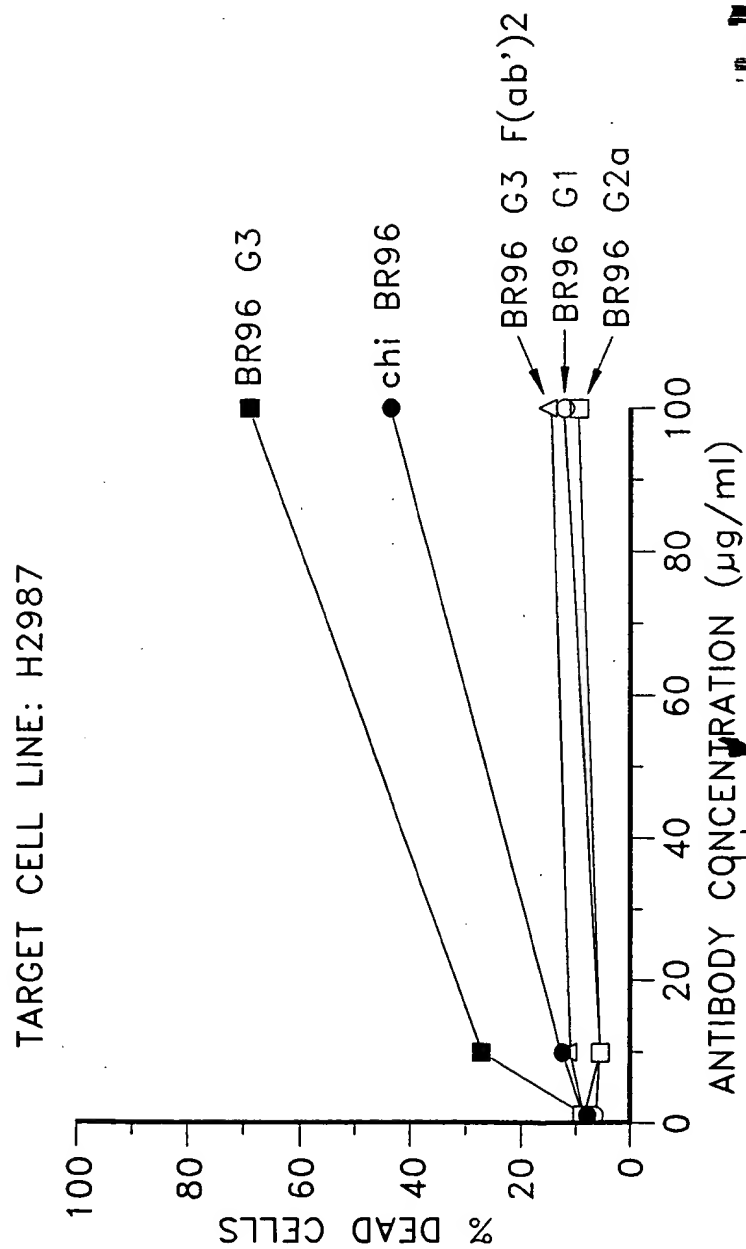


FIG. 19

55443 66433 66433 66433

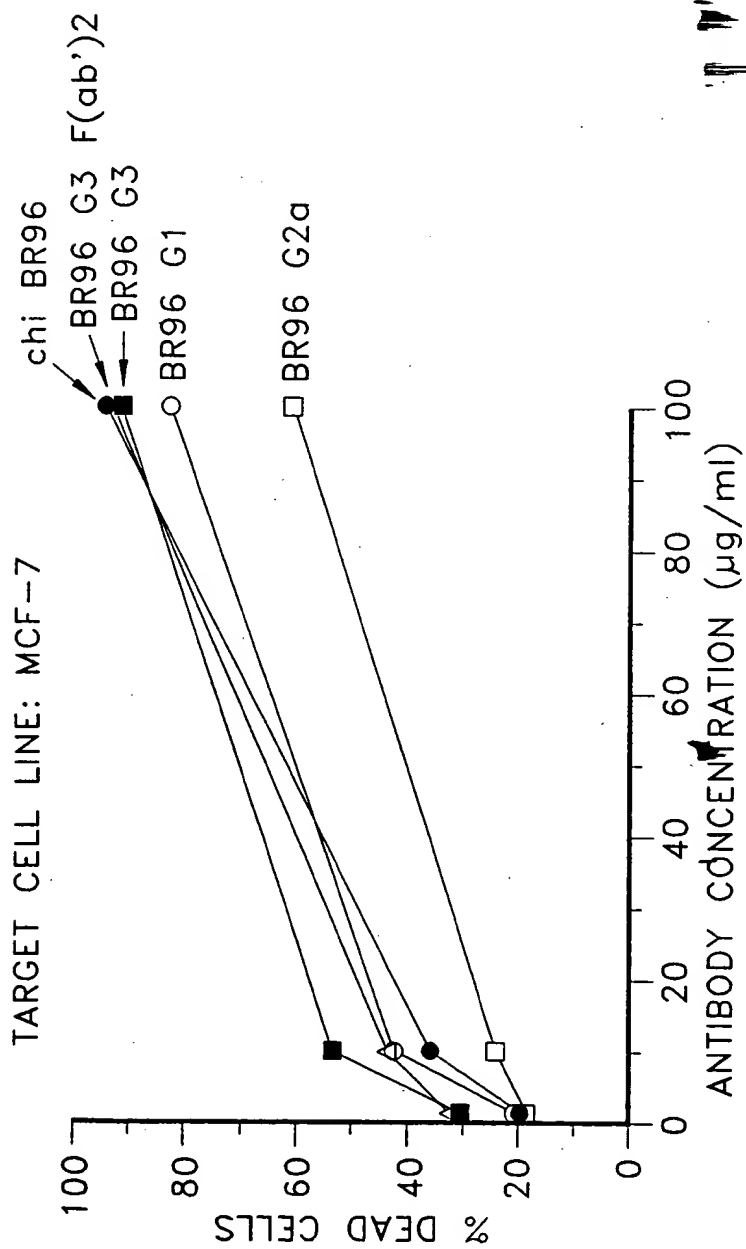


FIG. 20

664740-86205360

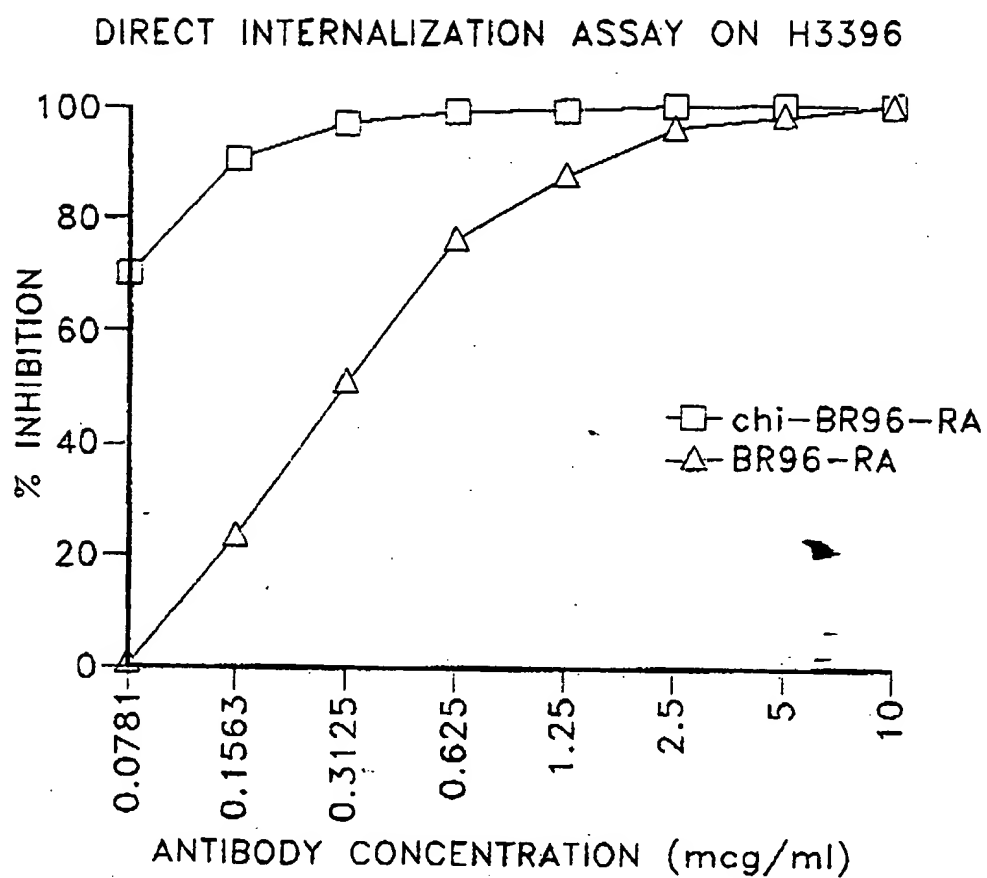


FIG. -21

6640-86253

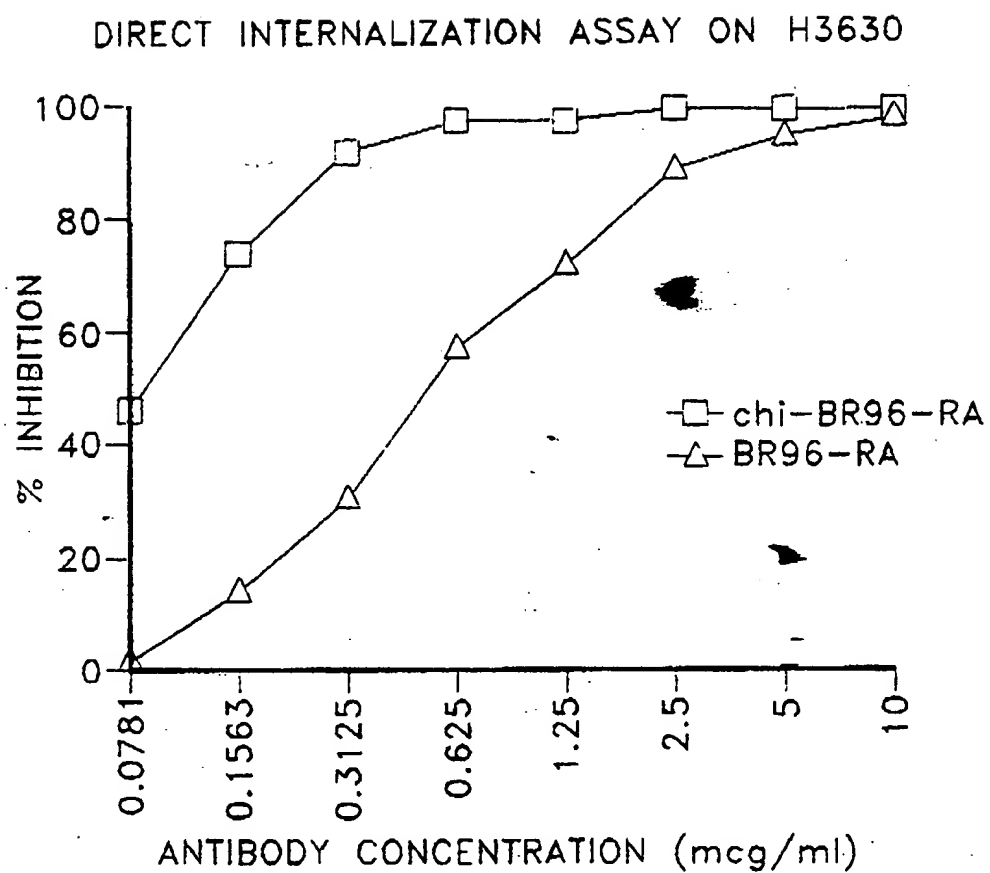


FIG. 22

666442-364360

EFFECTS OF UNMODIFIED Mabs ON H2987

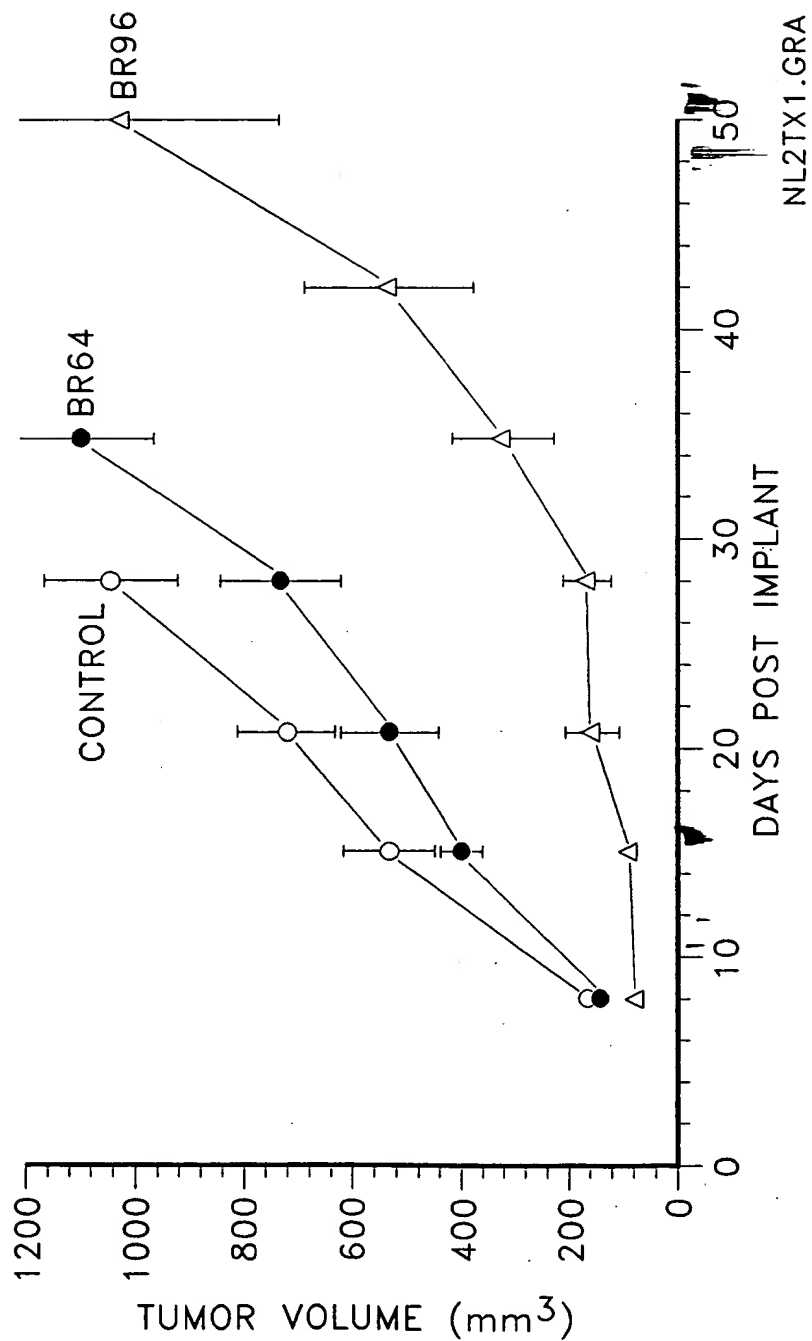


FIG. 23

ABSENCE OF TUMOR AT END OF TREATMENT
10 ANIMALS PER GROUP

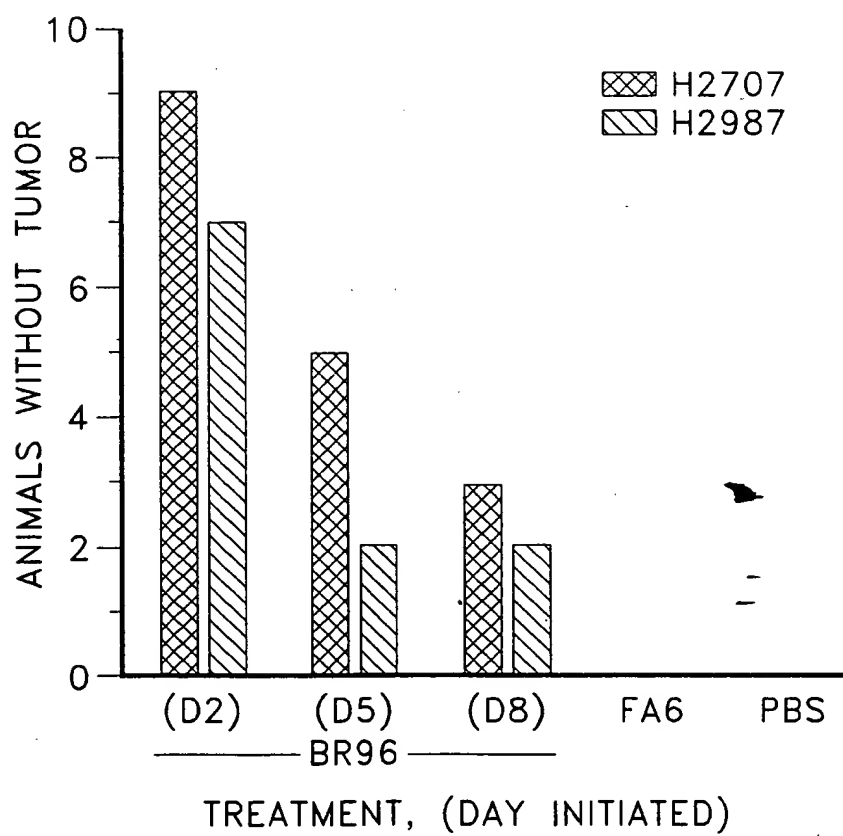


FIG. 24

66-44-6666

DOSE EFFECTS OF BR96 IgG3

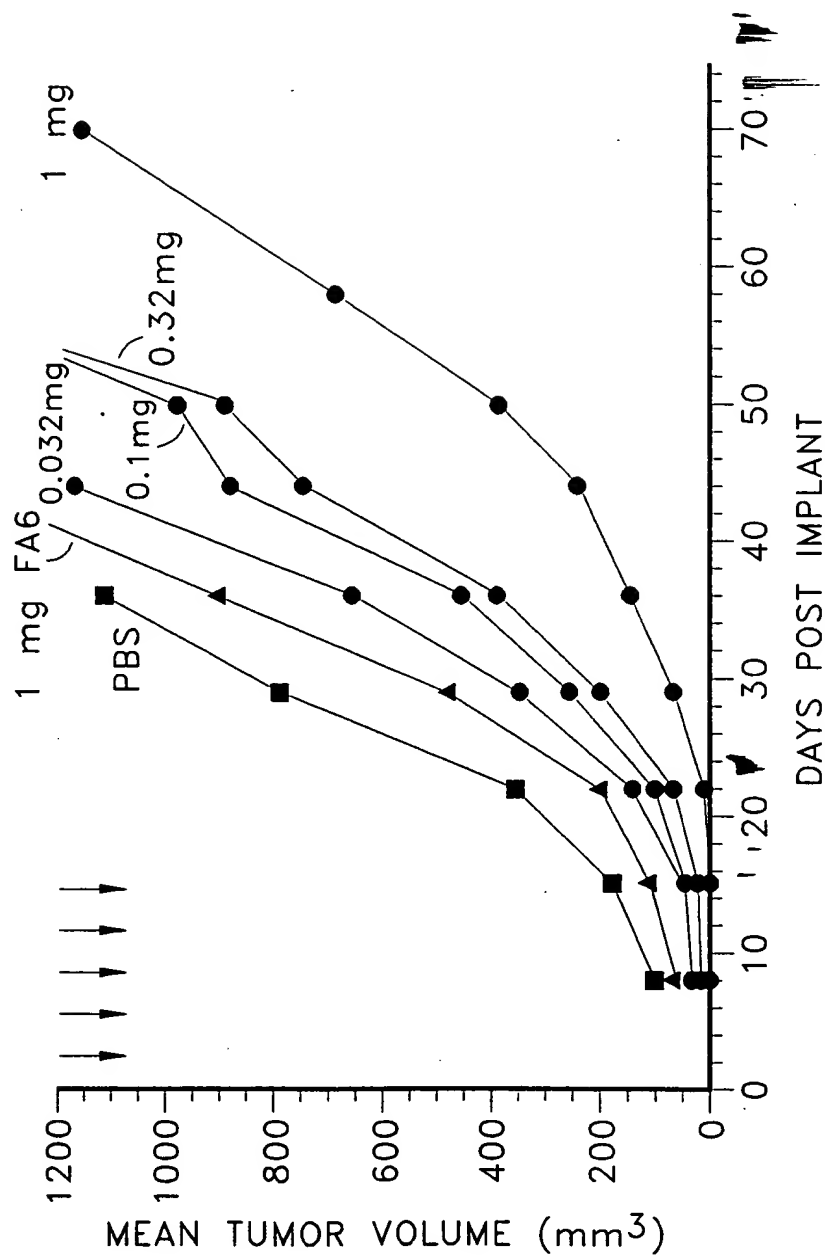


FIG. 25

EFFECTS OF F(ab')₂ AND CHIMERIC BR96 ON H2707

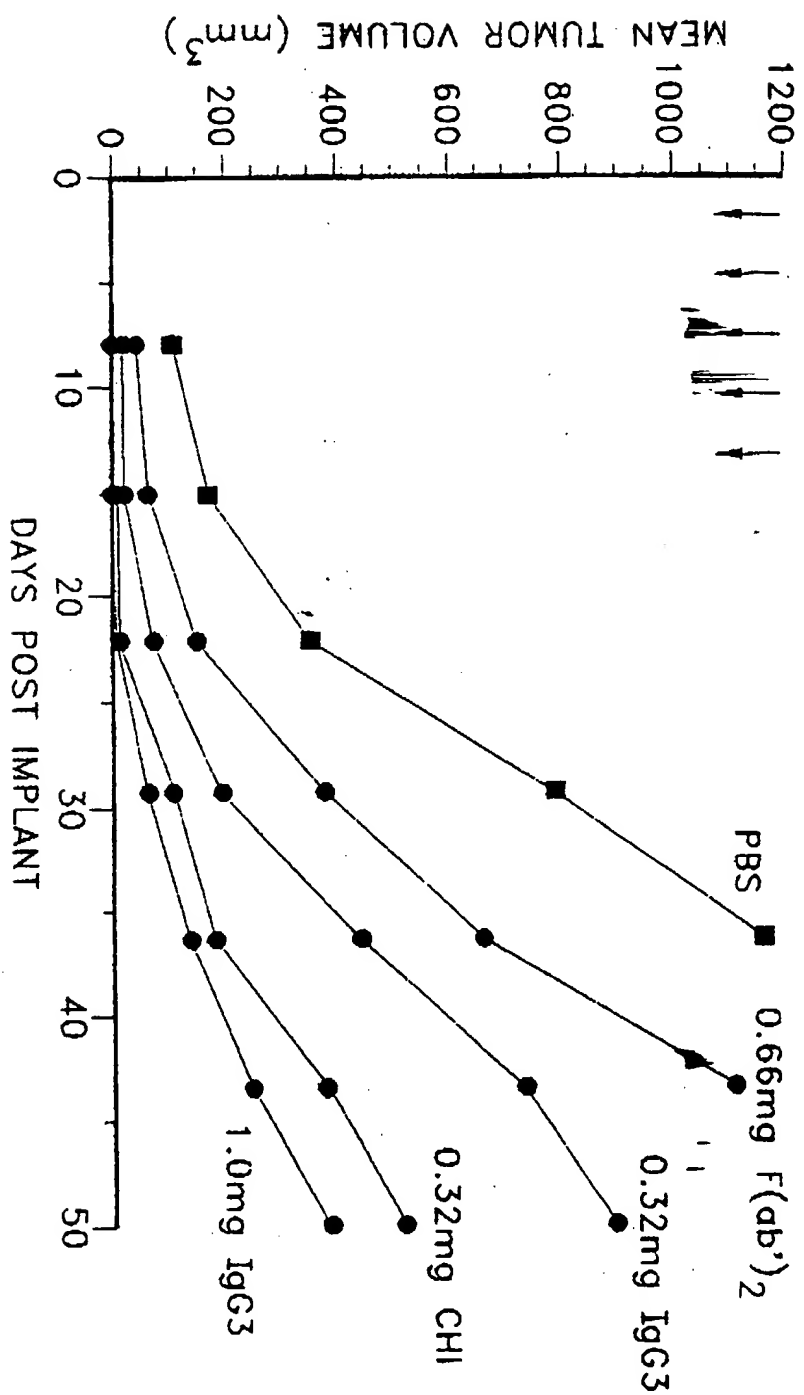


FIG. 26

ABSENCE OF TUMOR AFTER TREATMENT
8 ANIMALS PER GROUP
H2707 XENOGRAFT

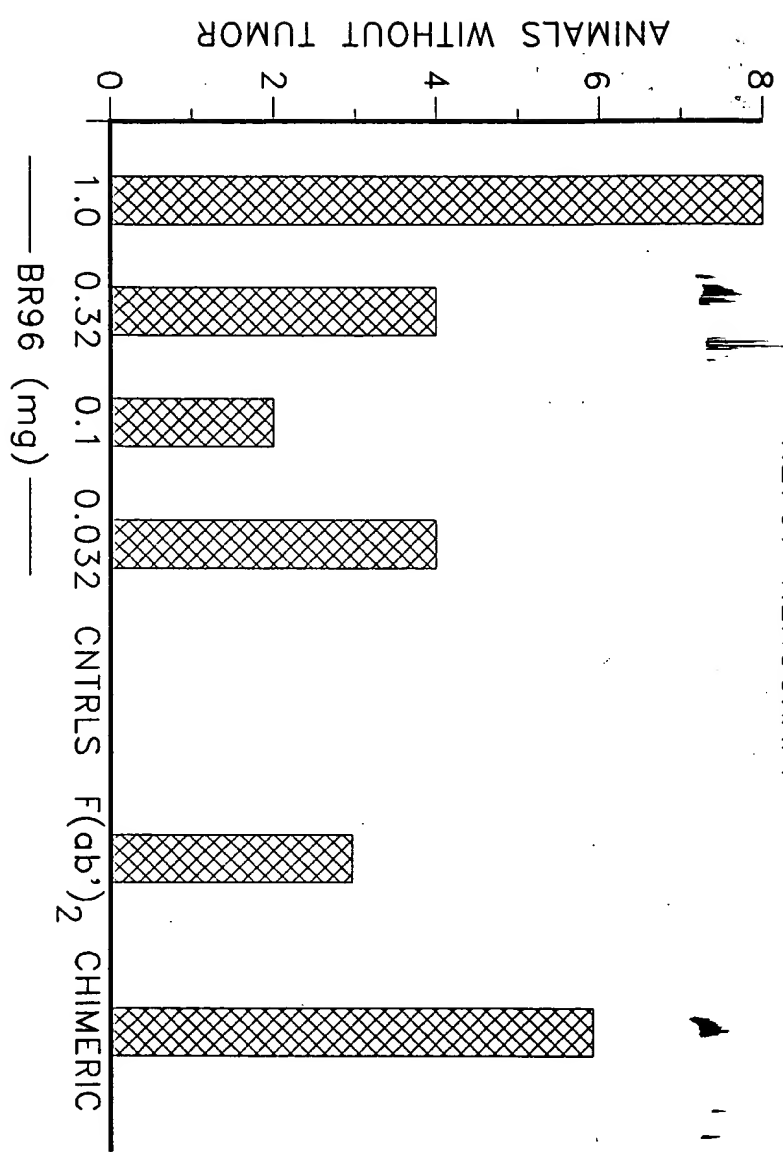


FIG. 27

000000-000000

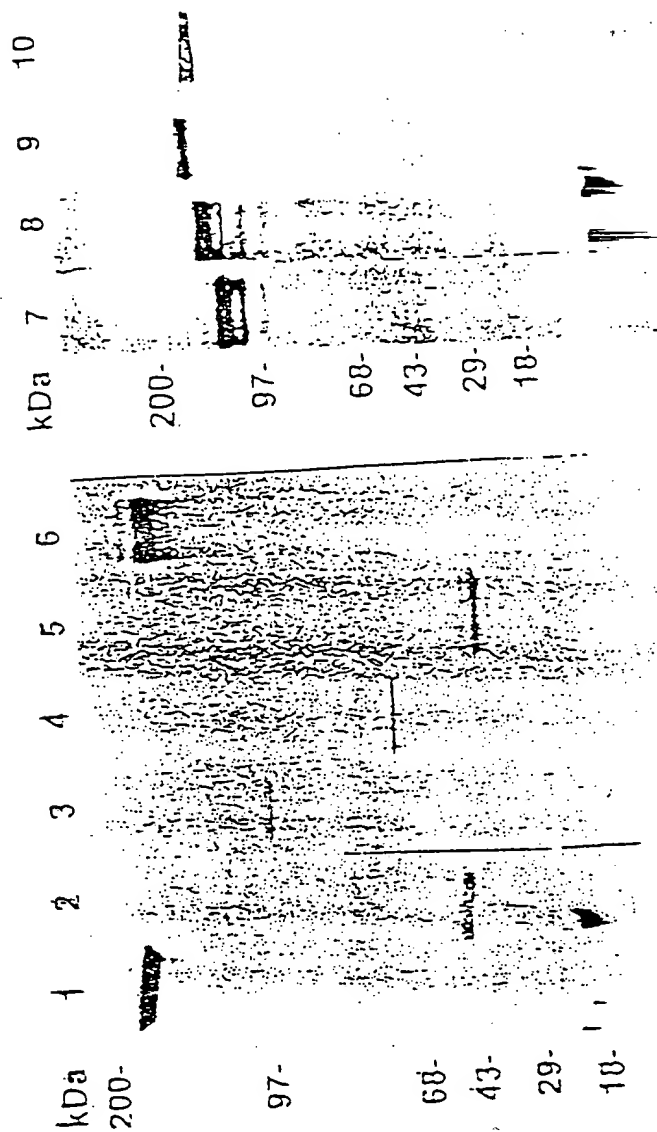


FIGURE 28

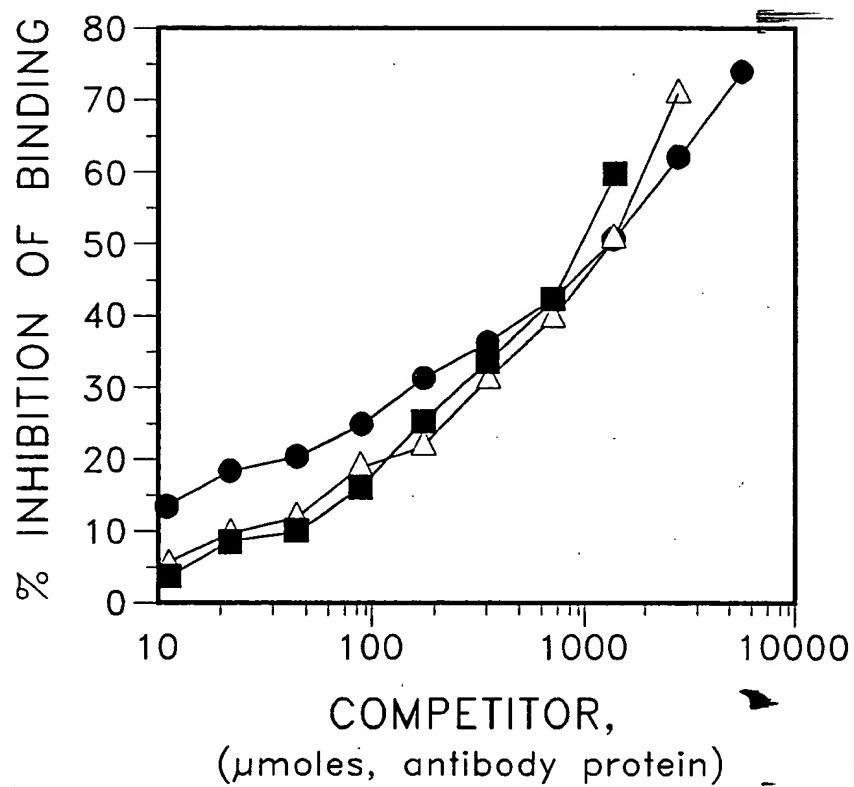


FIG. 29

66-44-6666

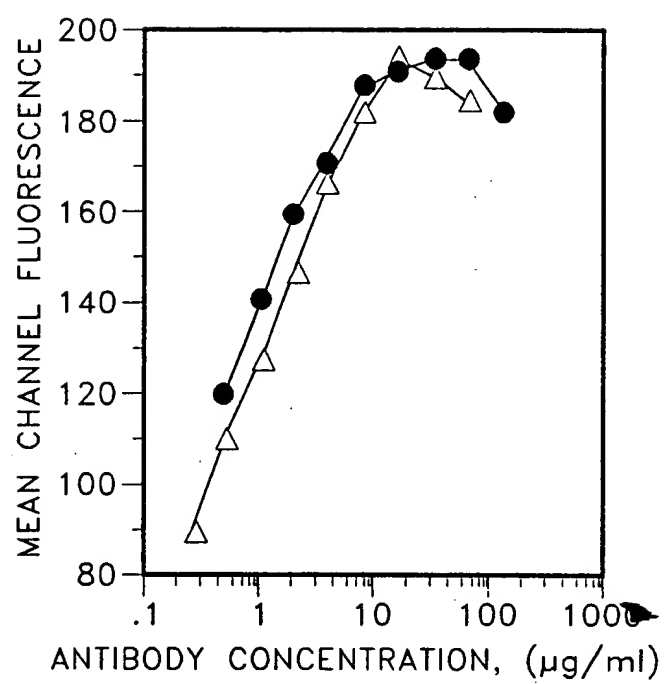


FIG. 30A

66740-862663

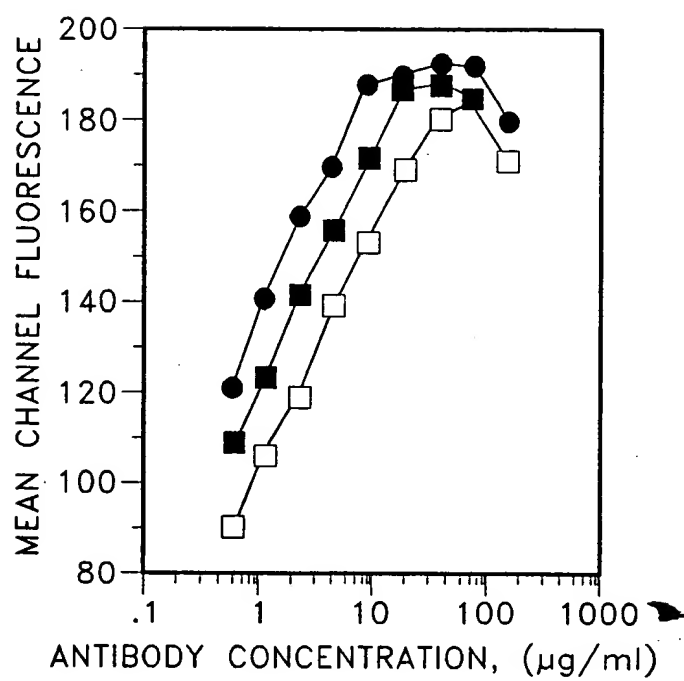


FIG. 30B

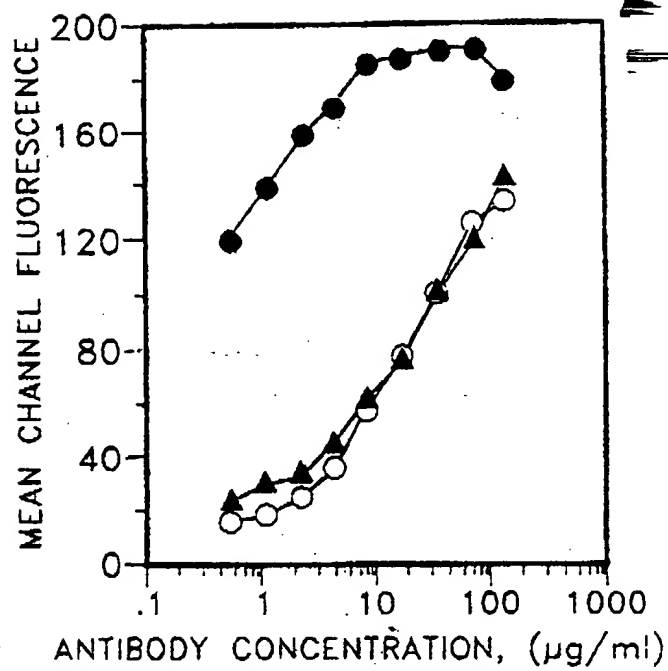


FIG. 30C

66740-66650

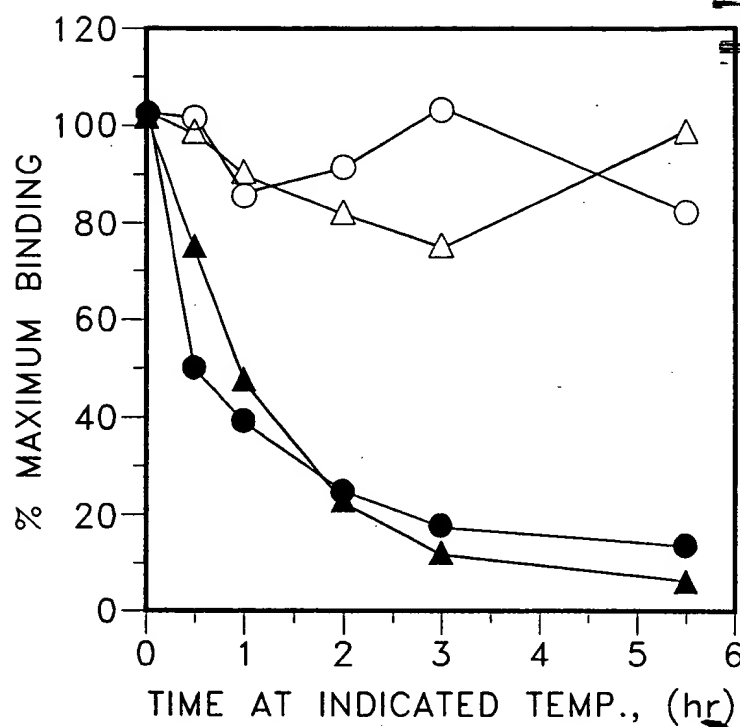


FIG. 31A

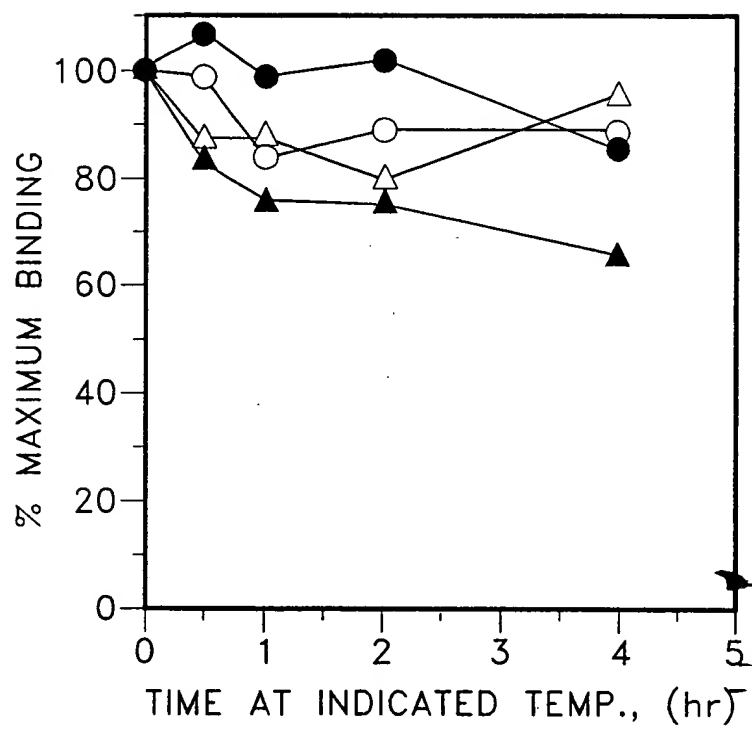


FIG. 31B

6640-26550

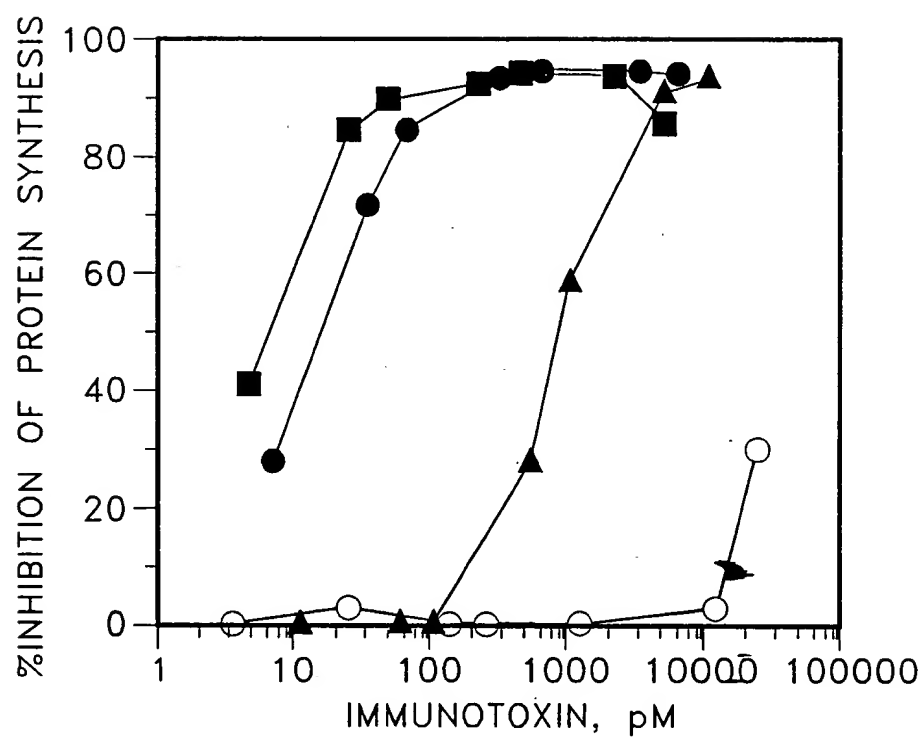


FIG. 32

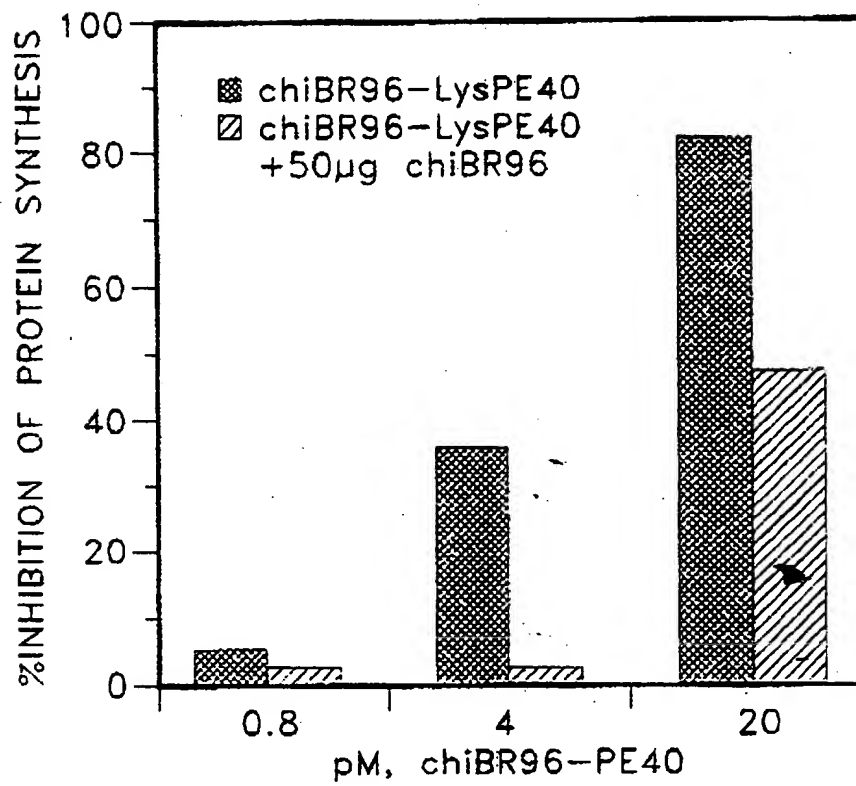


FIG. 33

66493-20000

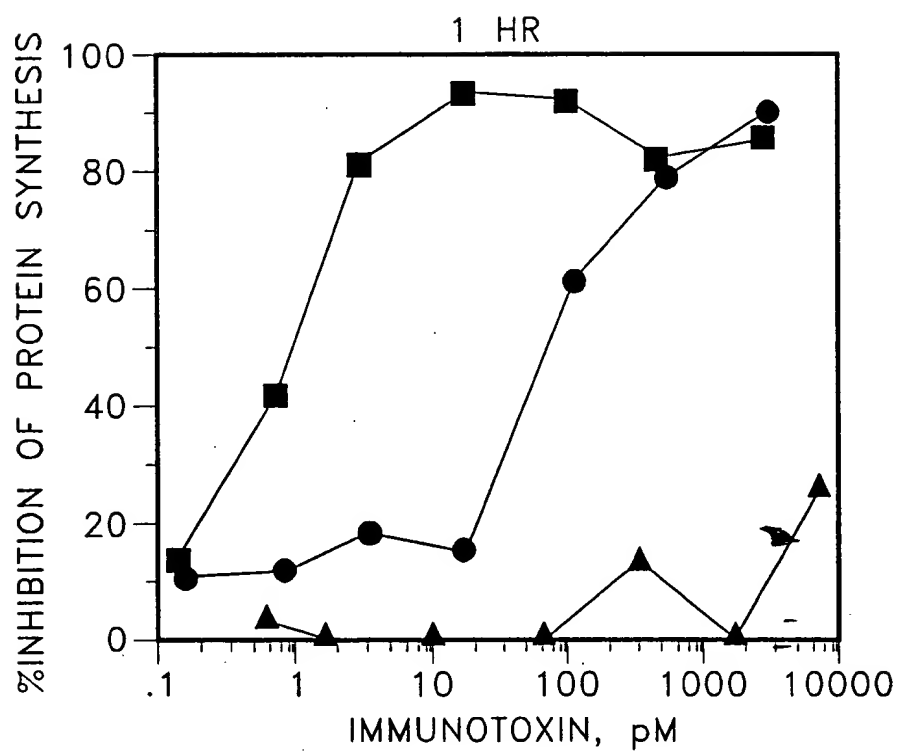


FIG. 34A

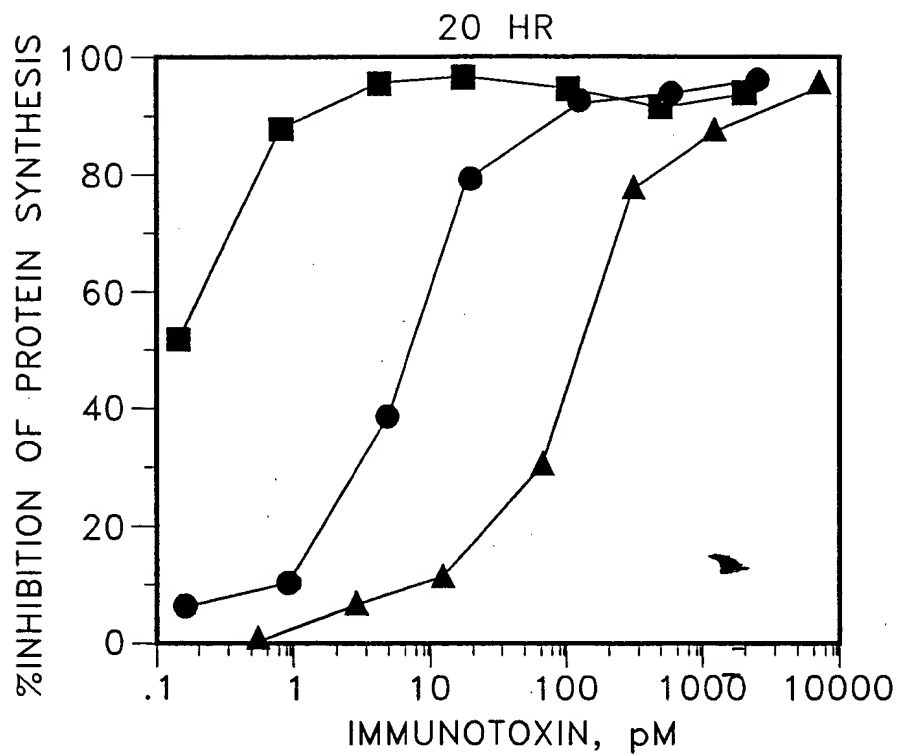


FIG. 34B

10	20	30	40
ATG GAG GTG CAG CTG GTG GAG TCT GGG GGA GGC TTA GTG CAG CCT GGG			
Met Glu Val Gln Leu Val Glu Ser Gly Gly Gly Leu Val Gln Pro Gly			
50	60	70	80
TCC CTG AAA GTC TCC TGT GTA ACC TCT GGA TTC ACT TTC AGT GAC TAT			
Ser Leu Lys Val Ser Cys Val Thr Ser Gly Phe Thr Phe Ser Asp Tyr			
100	110	120	130
TAC ATG TGG GTT CGC CAG ACT CCA GAG AAG AGG CTG GAG TGG GTC GCA			
Tyr Met Trp Val Arg Gln Thr Pro Glu Lys Arg Leu Glu Trp Val Ala			
150	160	170	180
TAC ATT AGT CAA GGT GAT ATA ACC GAC TAT CCA GAC ACT GTA AAG GGT			
Tyr Ile Ser Gln Gly Asp Ile Thr Asp Tyr Pro Asp Thr Val Lys Gly			
200	210	220	230
CGA TTC ACC ATC TCC AGA GAC AAT AAG AAC ACC CTG TAC CTG CAA ATG			
Arg Phe Thr Ile Ser Arg Asp Asn Lys Asn Thr Leu Tyr Leu Gln Met			
250	260	270	280
AGC CGT CTG AAG TCT GAG GAC ACA GCC ATG TAT TGT GCA AGA GGC CTG			
Ser Arg Leu Lys Ser Glu Asp Thr Ala Met Tyr Cys Ala Arg Gly Leu			
290	300	310	320
GAC GAC GGG GCC TGG TTT GCT TAC TGG GGC CAA GGG ACC ACG ACC GTC			
Asp Asp Gly Ala Trp Phe Ala Tyr Trp Gly Gln Gly Thr Thr Thr Val			
340	350	360	370
TCC TCA GGA TCC GGA GGT GGA GGT TCT GGT GGA GGT GGA TCT GGA GGT			
Ser Ser Gly Ser Gly Gly Gly Gly Ser Gly Gly Gly Gly Ser Gly Gly			
390	400	410	420
GGA TCT AAG CTT GAT GTT TTG ATG ACC CAA ATT CCA GTC TCC CTG CCT			
Gly Ser Lys Leu Asp Val Leu Met Thr Gln Ile Pro Val Ser Leu Pro			
440	450	460	470
GTC AGT CTT GGA CAA GCG TCC ATC TCT TGC AGA TCT AGT CAG ATC ATT			
Val Ser Leu Gly Gln Ala Ser Ile Ser Cys Arg Ser Ser Gln Ile Ile			

66E440 = 66E440

490	500	510	520
GTA CAT AAT AAT GGC AAC ACC TTA GAA TGG TAC CTG CAG AAA CCA GGC			
Val His Asn Asn Gly Asn Thr Leu Glu Trp Tyr Leu Gln Lys Pro Gly			
530	540	550	560
CAG TCT CCA CAG CTC CTG ATC TAC AAA GTT AAC CGA TTT TCT GGG GTC			
Gln Ser Pro Gln Leu Leu Ile Tyr Lys Val Asn Arg Phe Ser Gly Val			
580	590	600	610
CCA GAC AGG TTC AGC GGC AGT GGA TCA GGG ACA GAT TTC CTC AAG ATC			
Pro Asp Arg Phe Ser Gly Ser Gly Ser Gly Thr Asp Phe Leu Lys Ile			
630	640	650	660
AGC AGA GTG GAG GCT GAG GAT CTG GGA GTT TAT TAC TGC TTT CAA GTT			
Ser Arg Val Glu Ala Glu Asp Leu Gly Val Tyr Tyr Cys Phe Gln Val			
680	690	700	710
CAT GTT CCA TTC ACG TTC GGC TCG GGG ACC AAG CTG GAG ATC AAA CGC			
His Val Pro Phe Thr Phe Gly Ser Gly Thr Lys Leu Glu Ile Lys Arg			
720			

Figure 35 (Cont.)

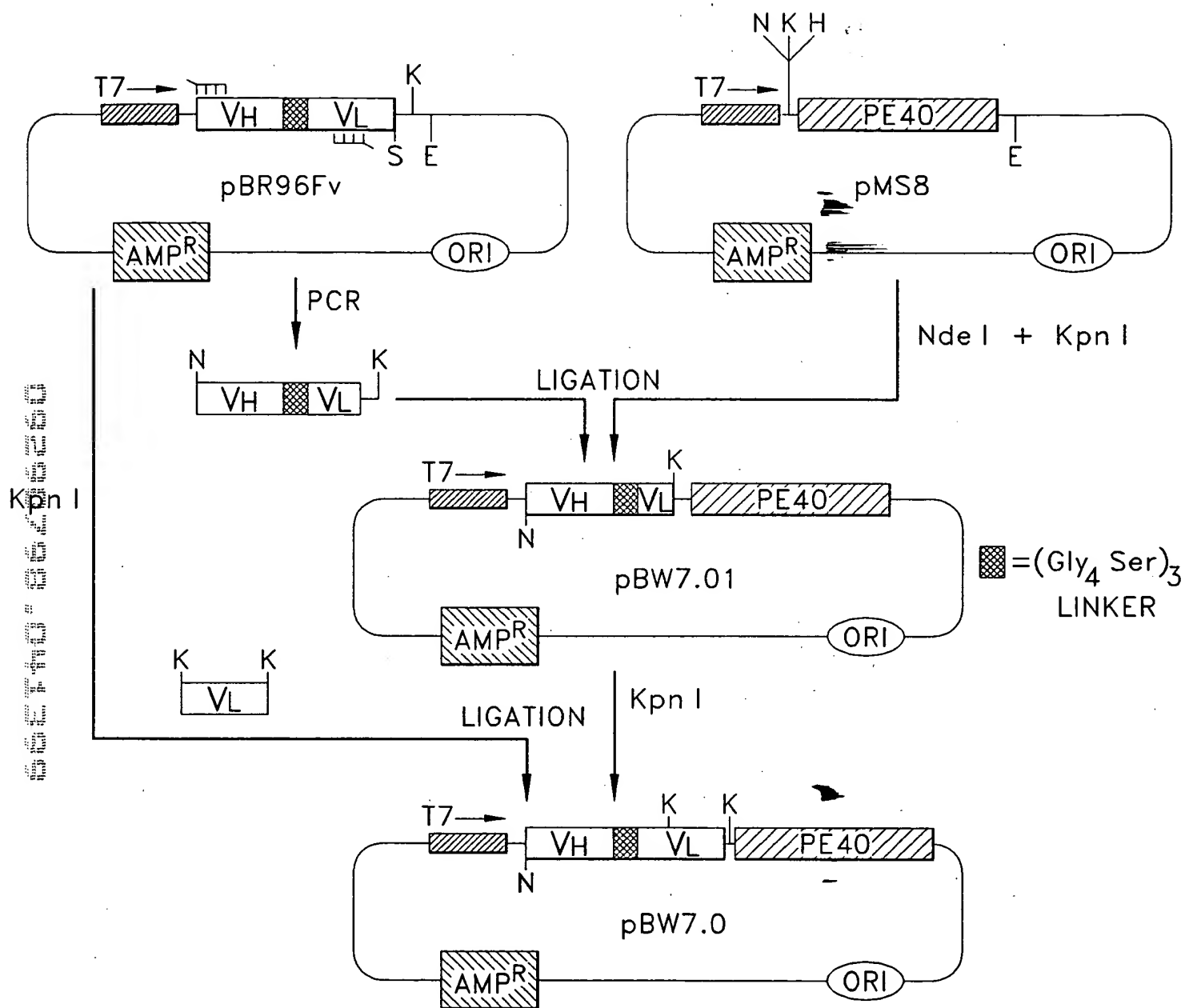


FIG. 36

66403320600

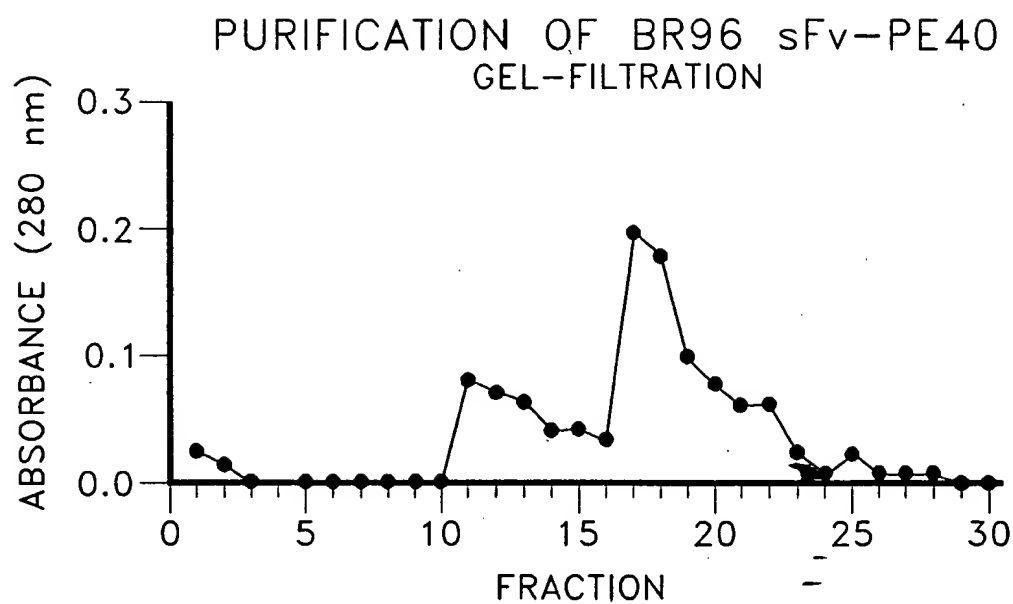


FIG. 37A.

Figure 37 B.

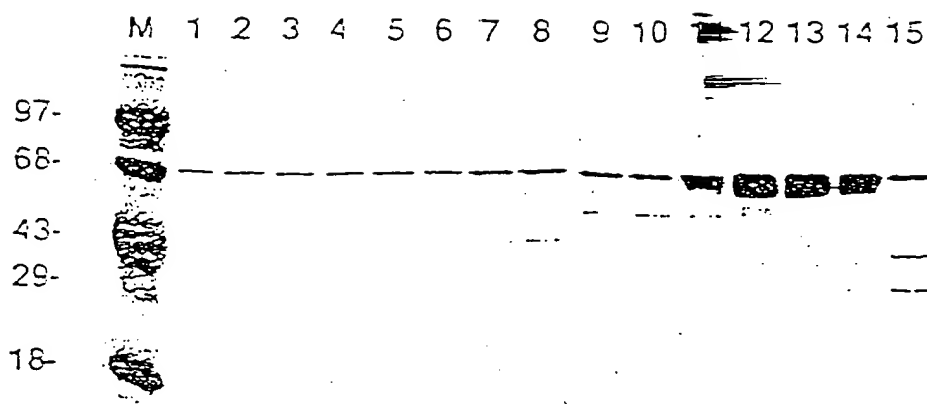
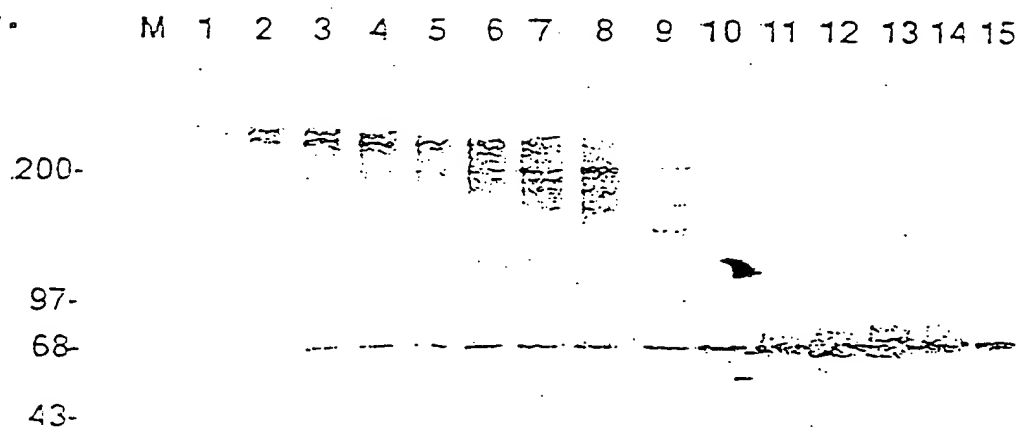


Figure 37 C.



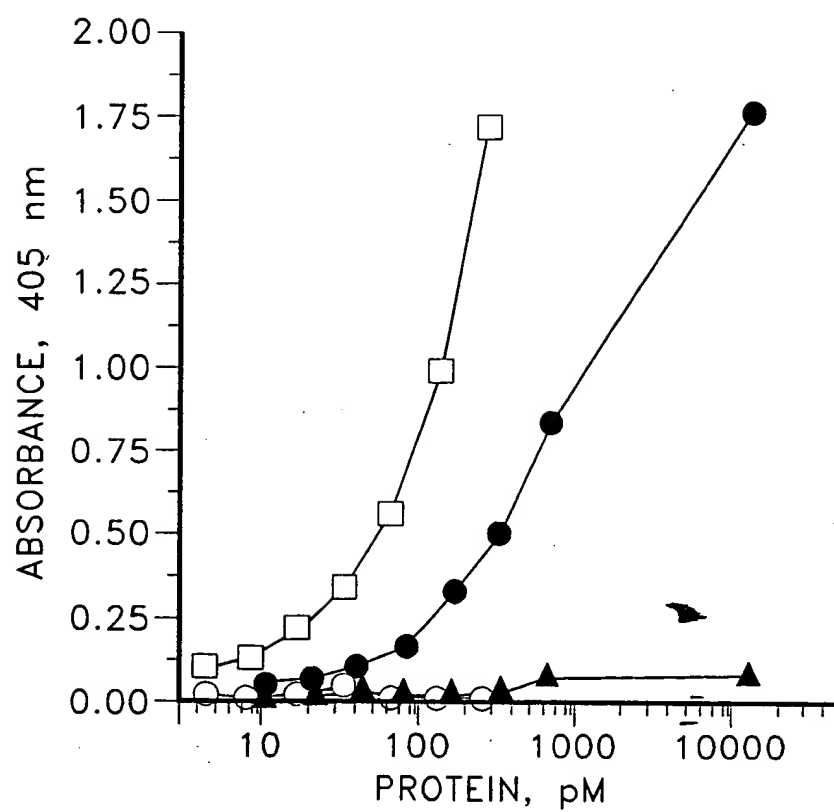


FIG. 38

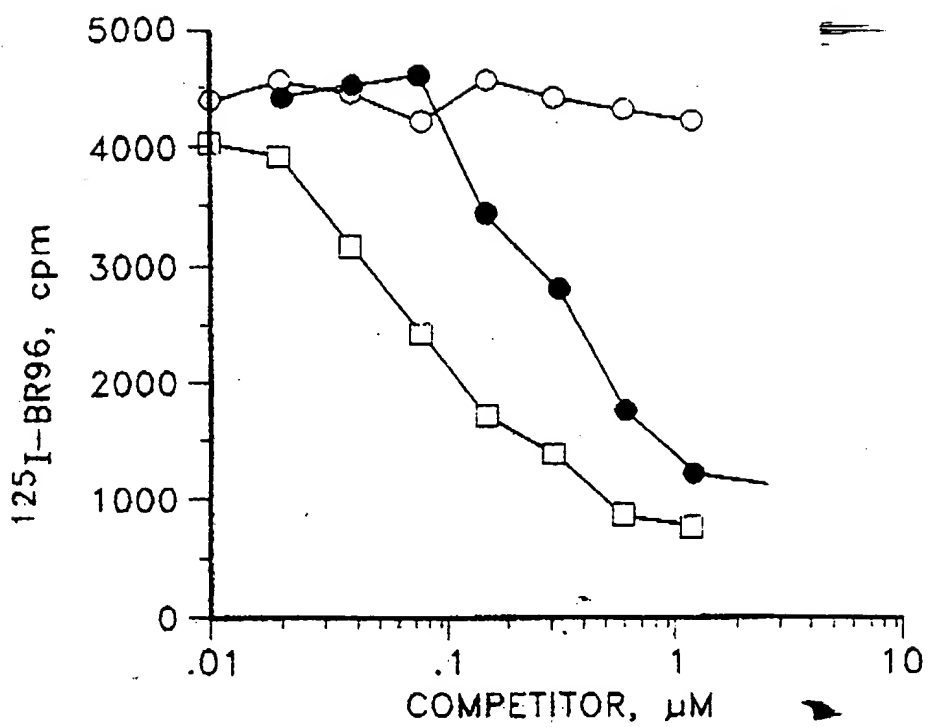


FIG. 39

65-140-8605-5

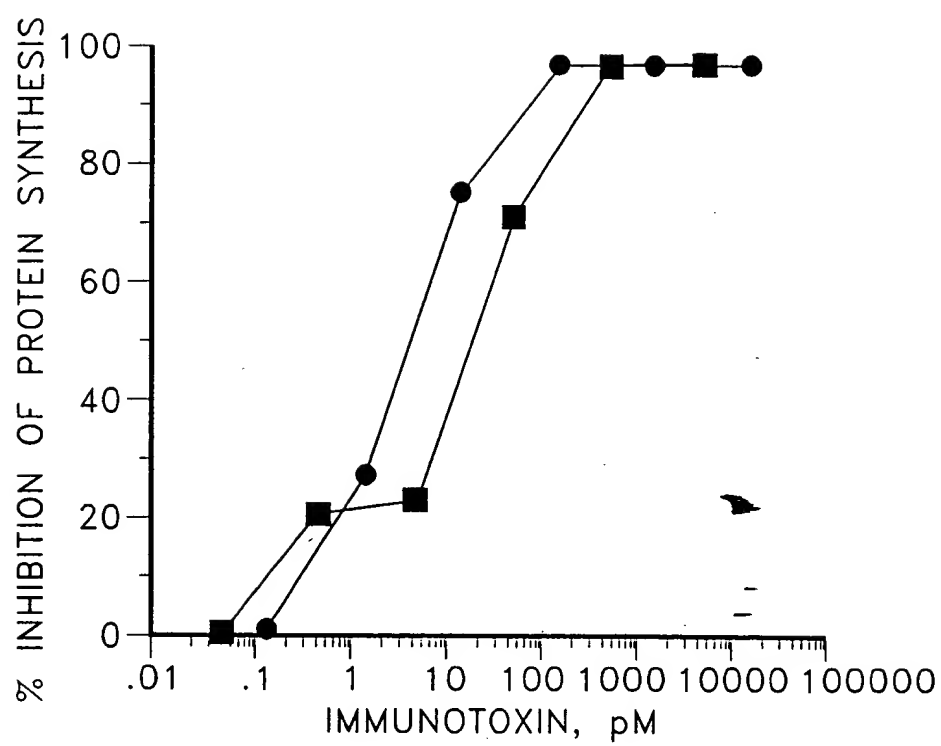


FIG. 40

Human IgG

Chimeric BR96

KB

2.7

36.3

A2780

1.6

104.8

RCA

7.6

146.1

L2987

3.9

176.7

MCF7

2.5

180.3

FIGURE 41

66-44-88208266

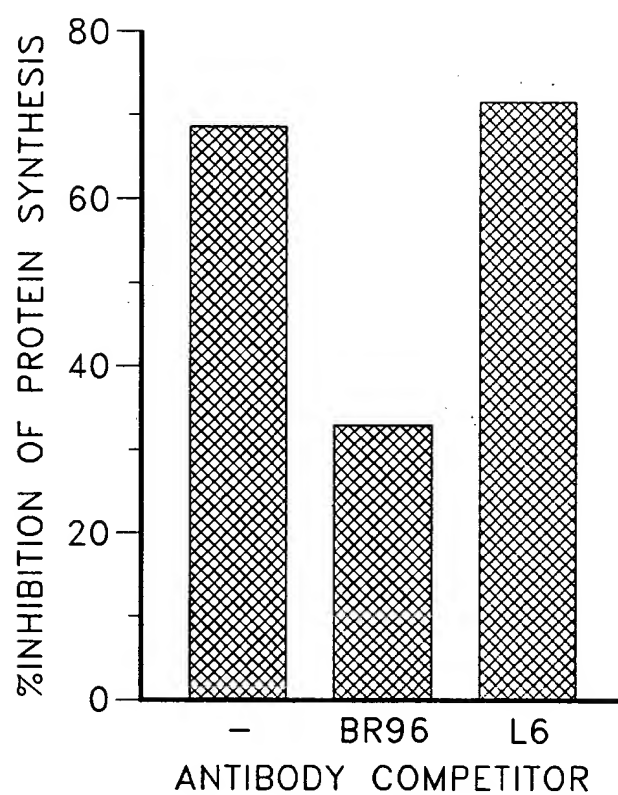


FIG. 42

MCF7 HUMAN BREAST TUMOR XENOGRAFT
BR96 sFv-PE40 TREATMENT STARTED ON d12

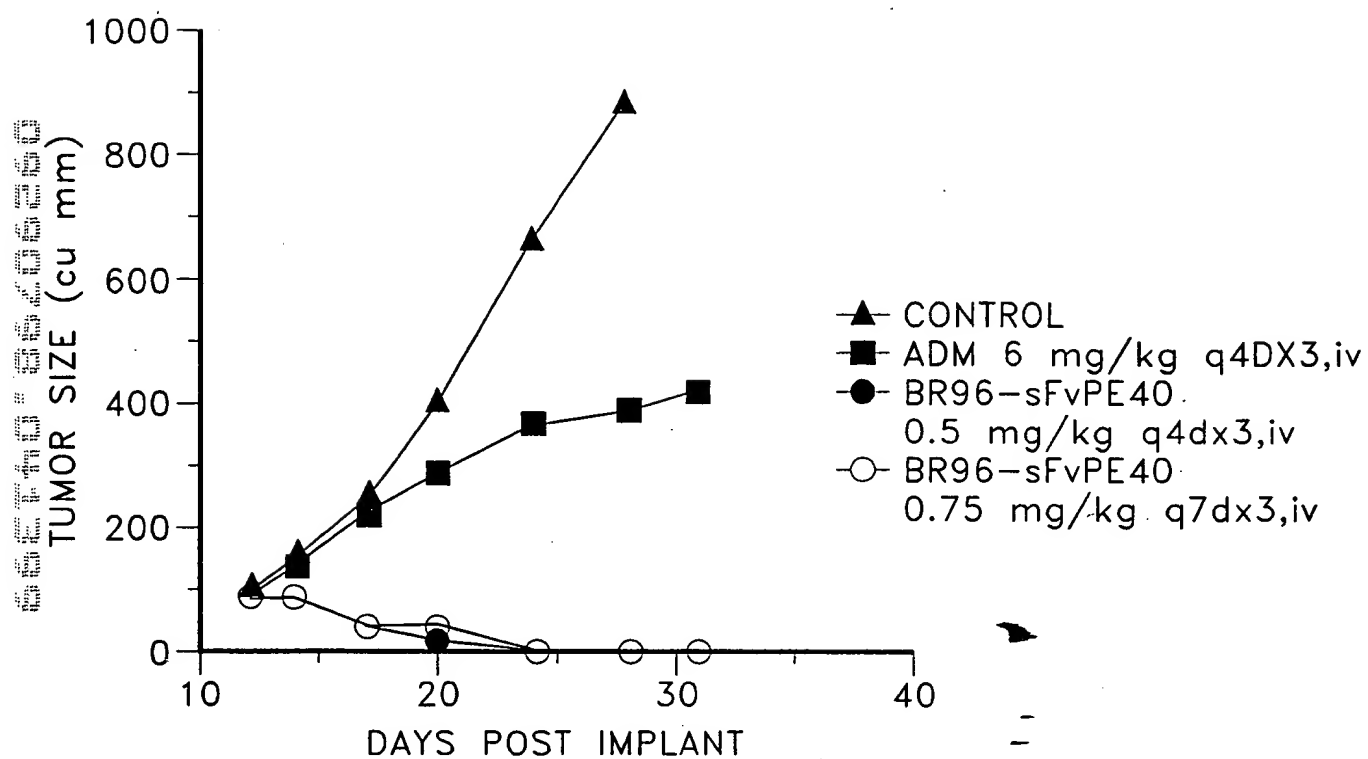


FIG. 43

ANTI-TUMOR ACTIVITY OF BR96-IMMUNOTOXINS AGAINST L2987 HUMAN LUNG TUMOR XENOGRAFTS

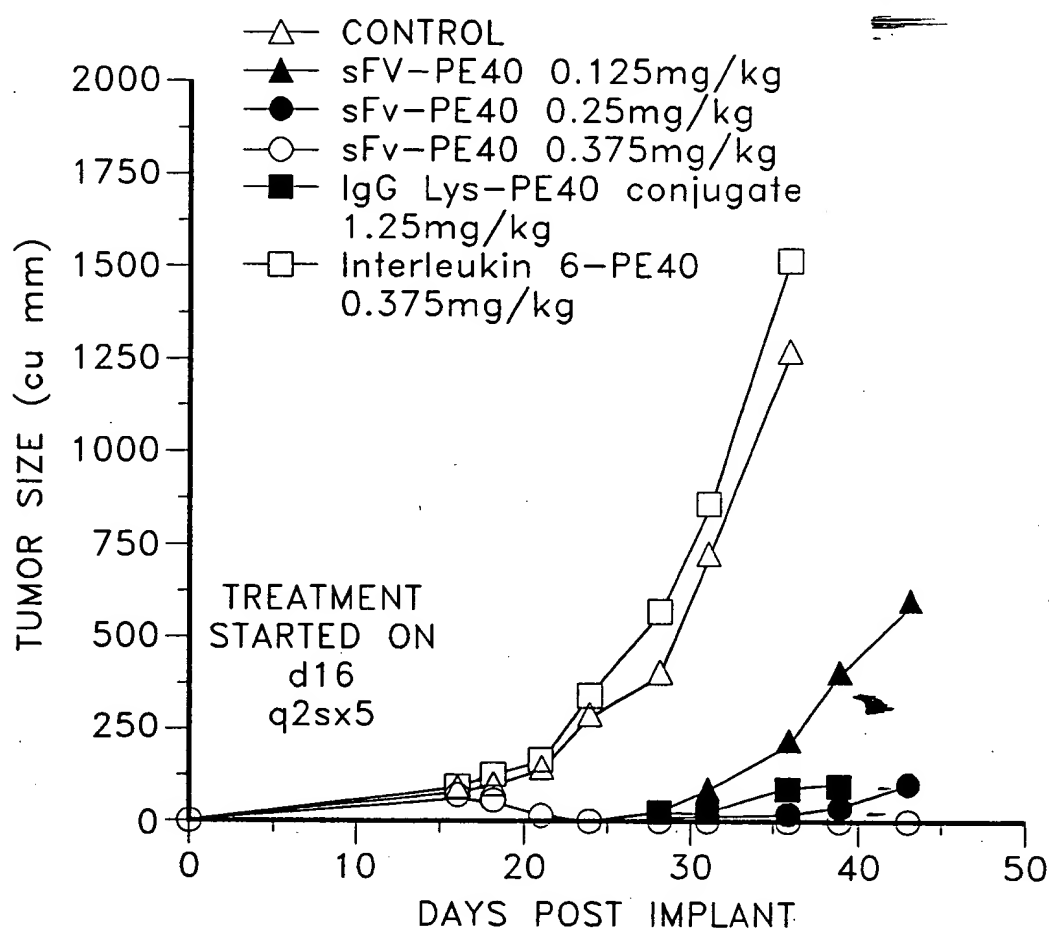


FIG. 44

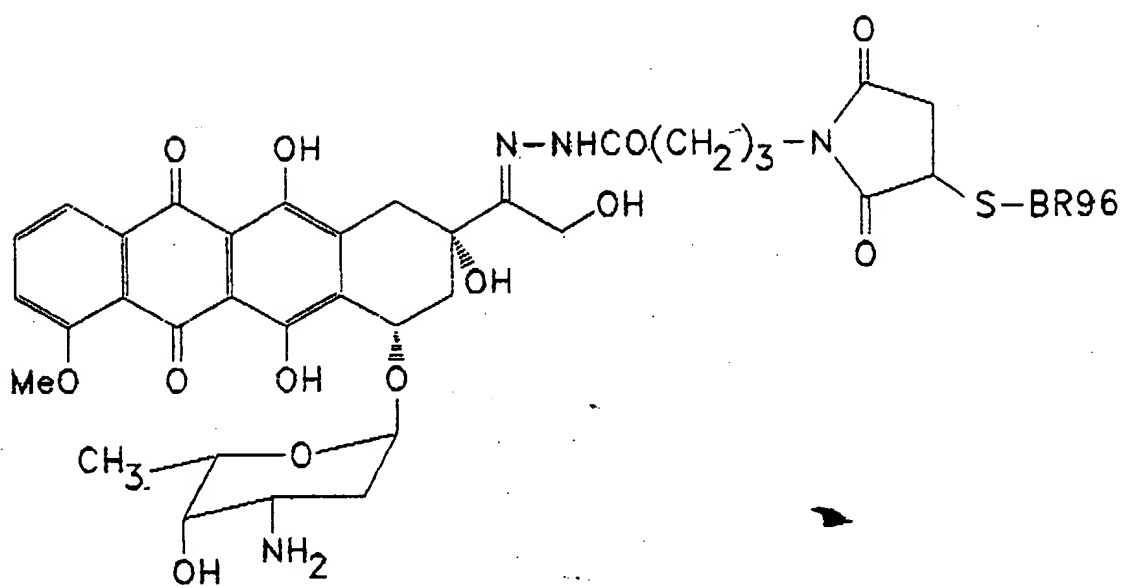


FIG. 45

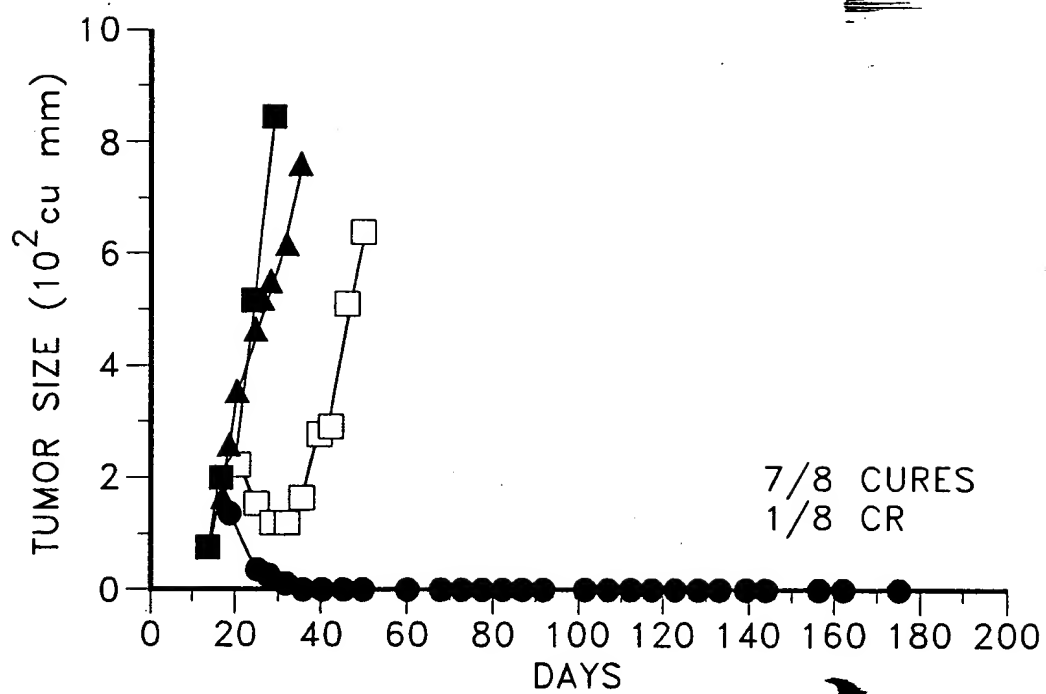


FIG. 46A

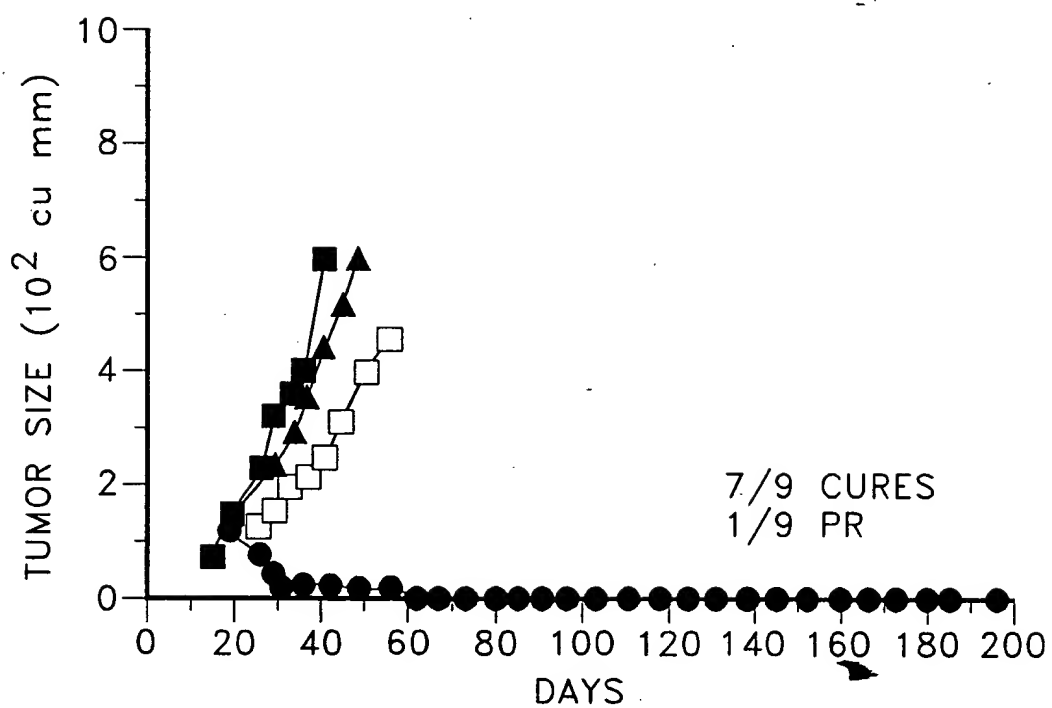


FIG. 46B

66-40-86-80

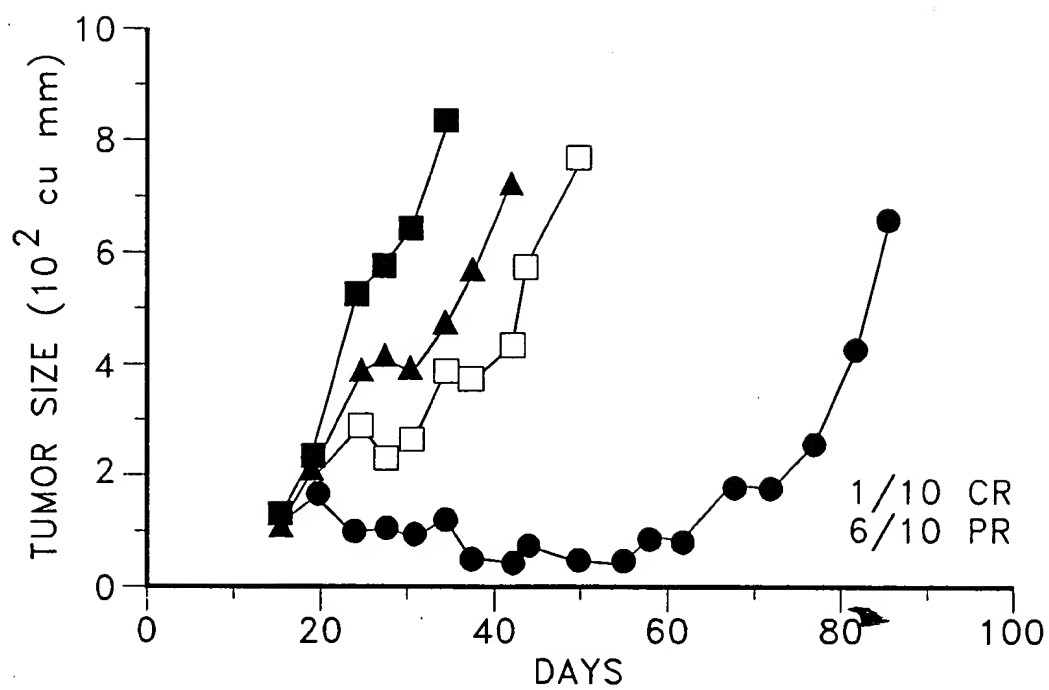


FIG. 46C

SECRET

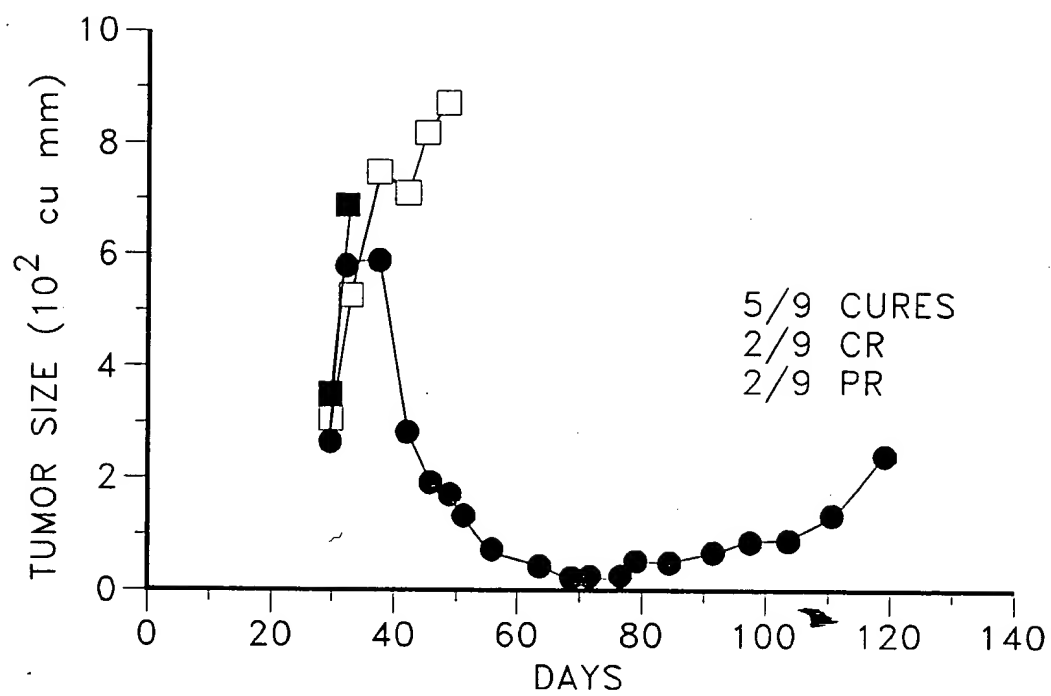


FIG. 46D

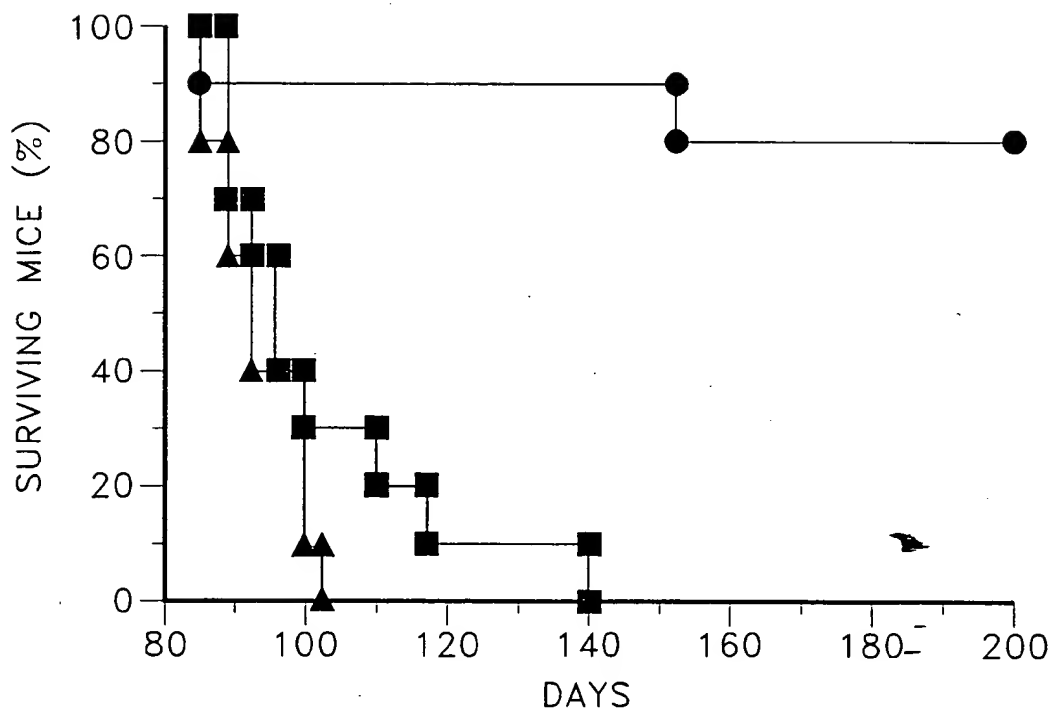


FIG. 47

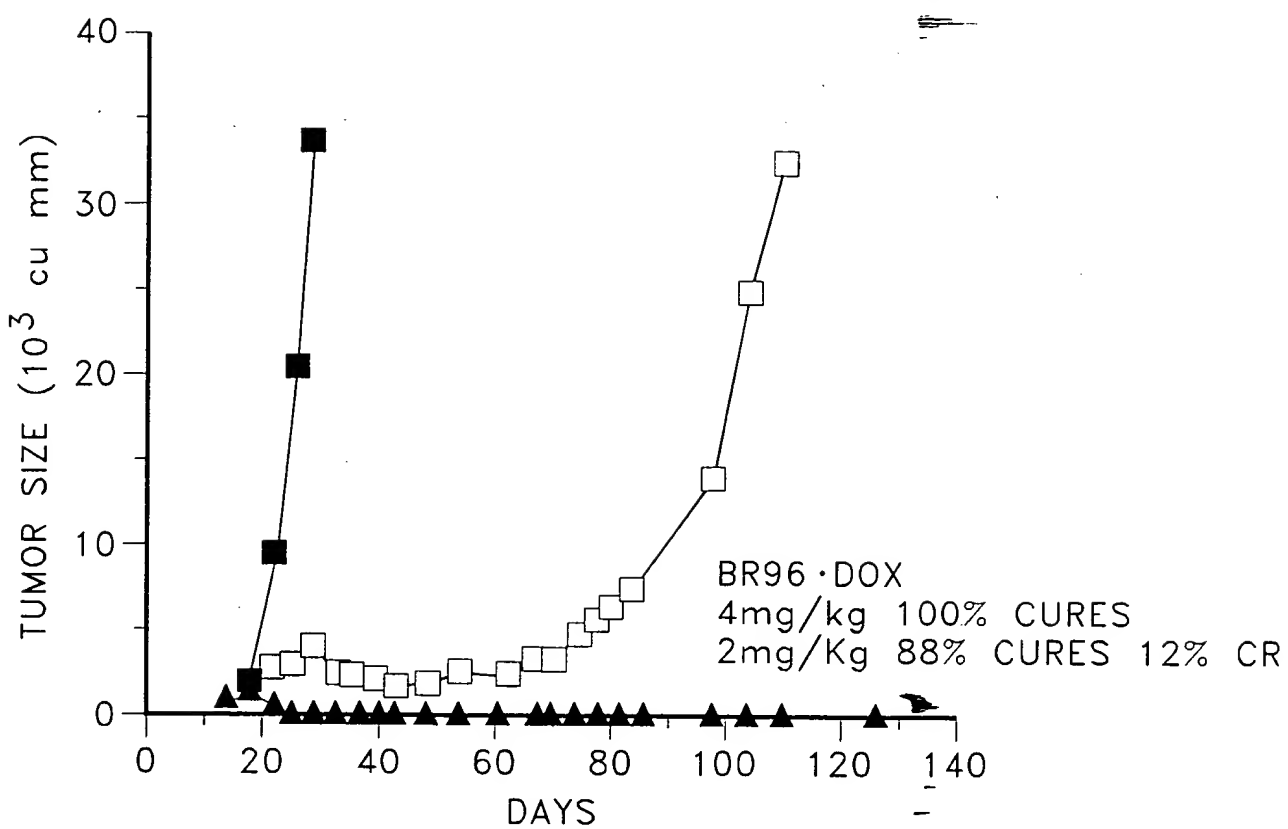


FIG. 48

FIGURE 49a

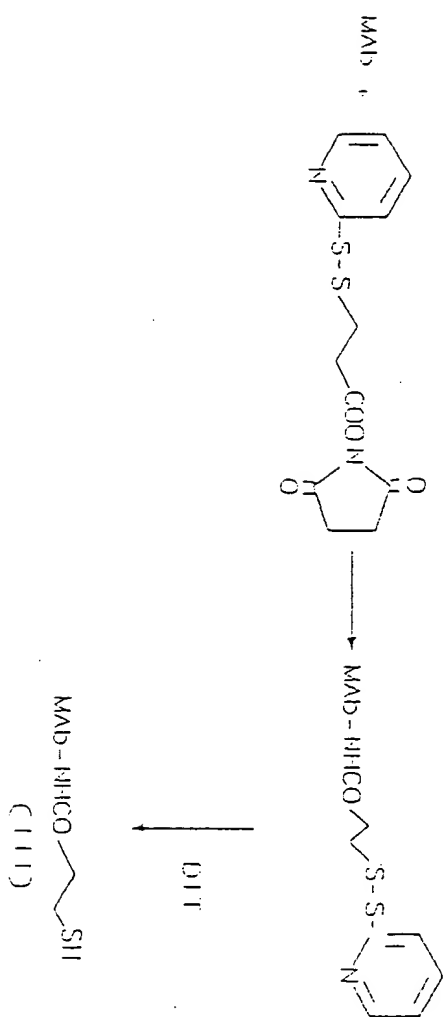


FIGURE 49b

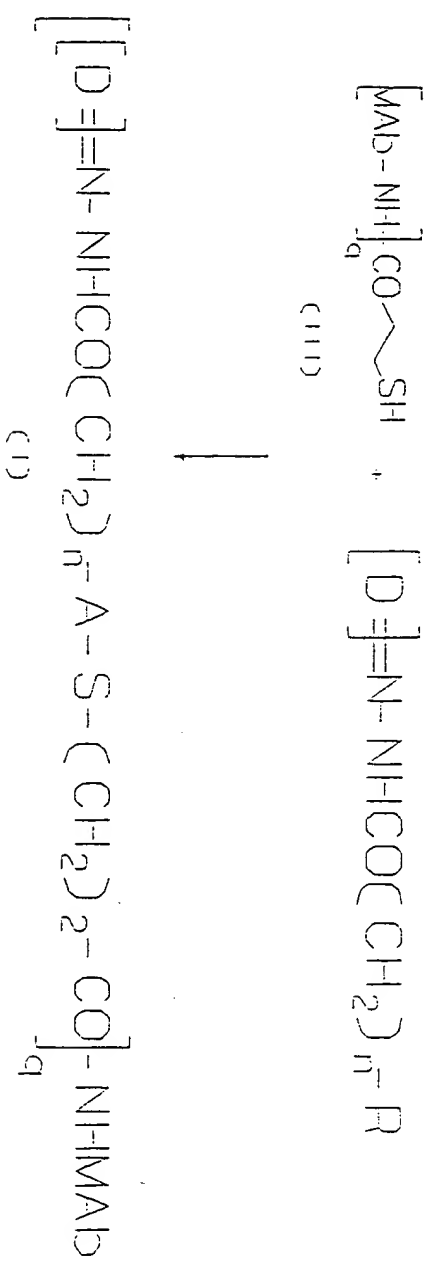


FIGURE 49c

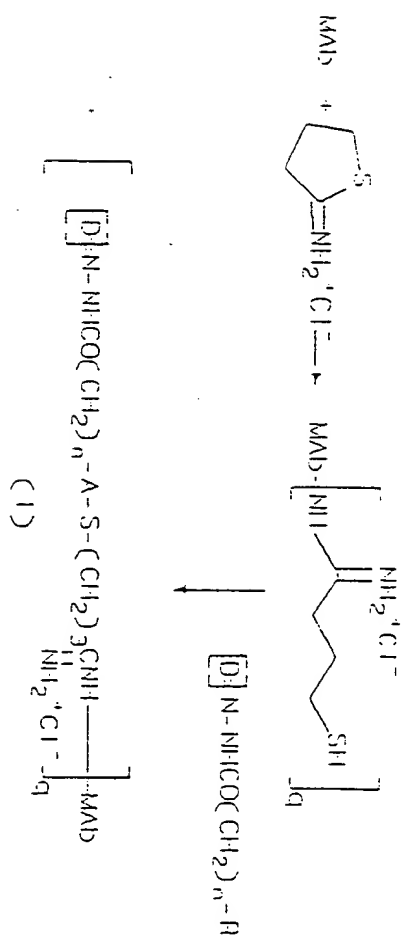
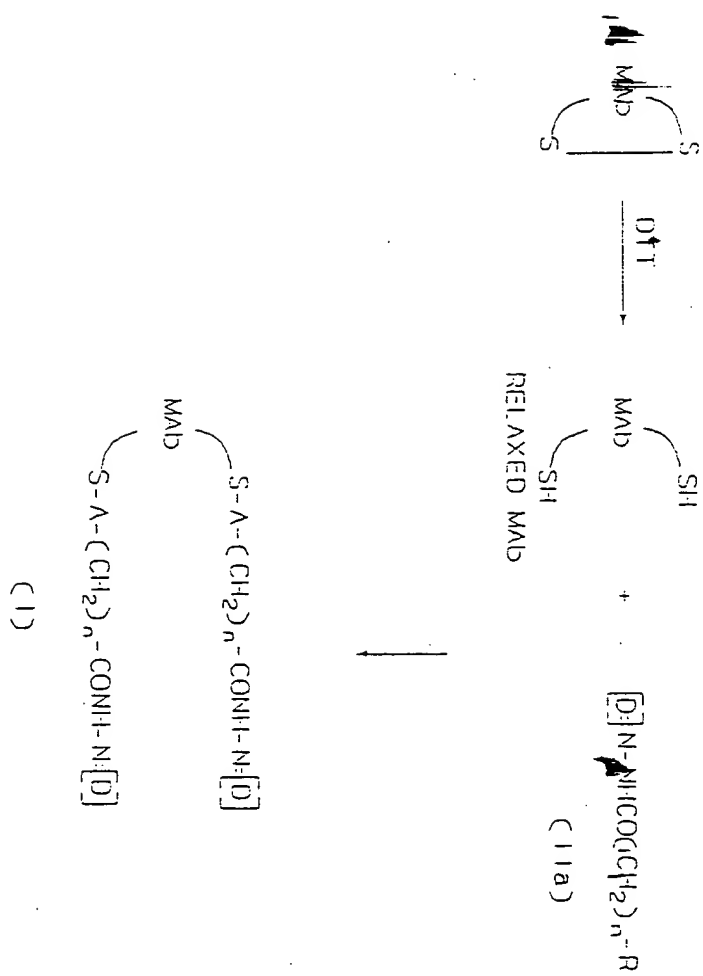
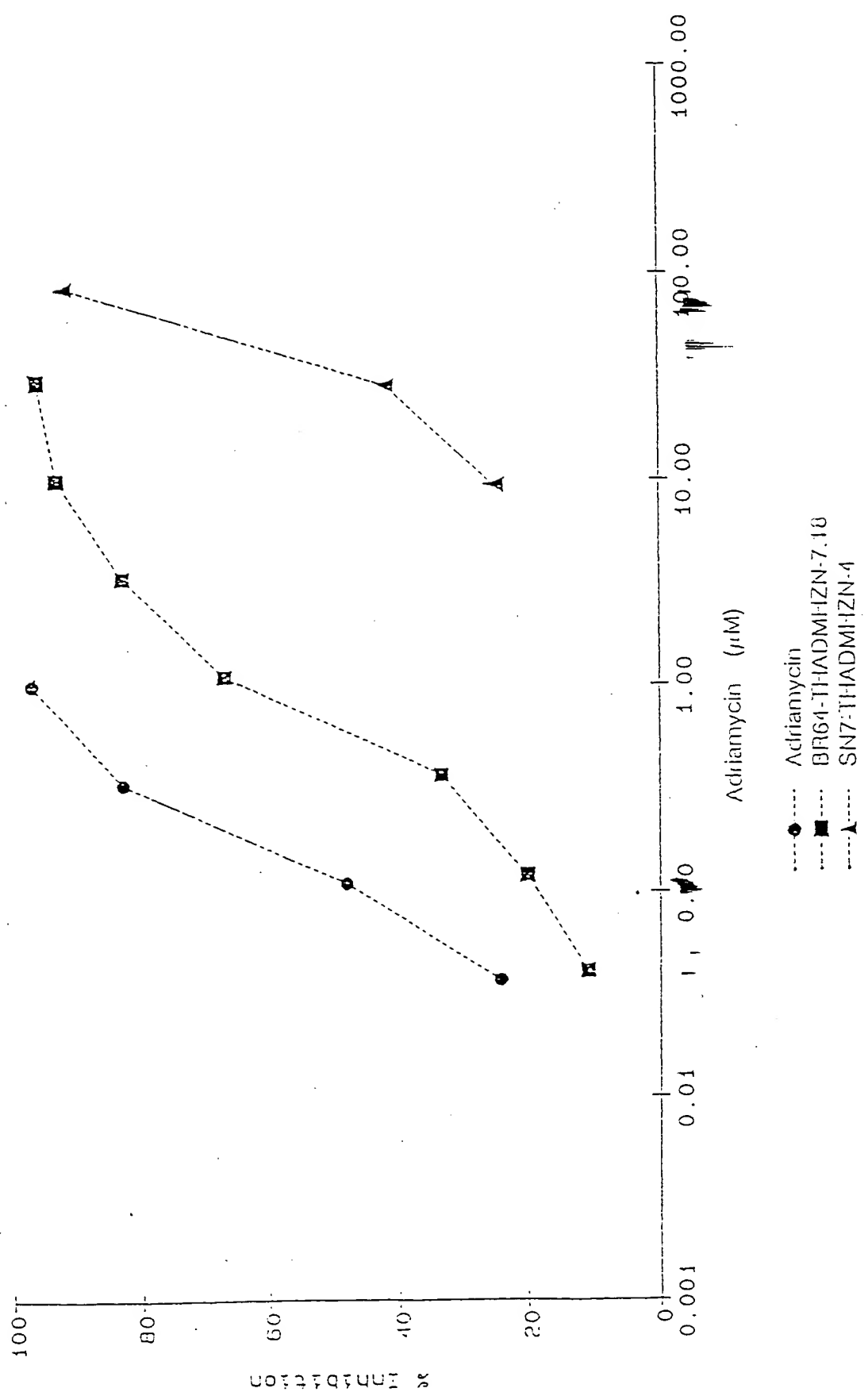


FIGURE 50



Cell Proliferation

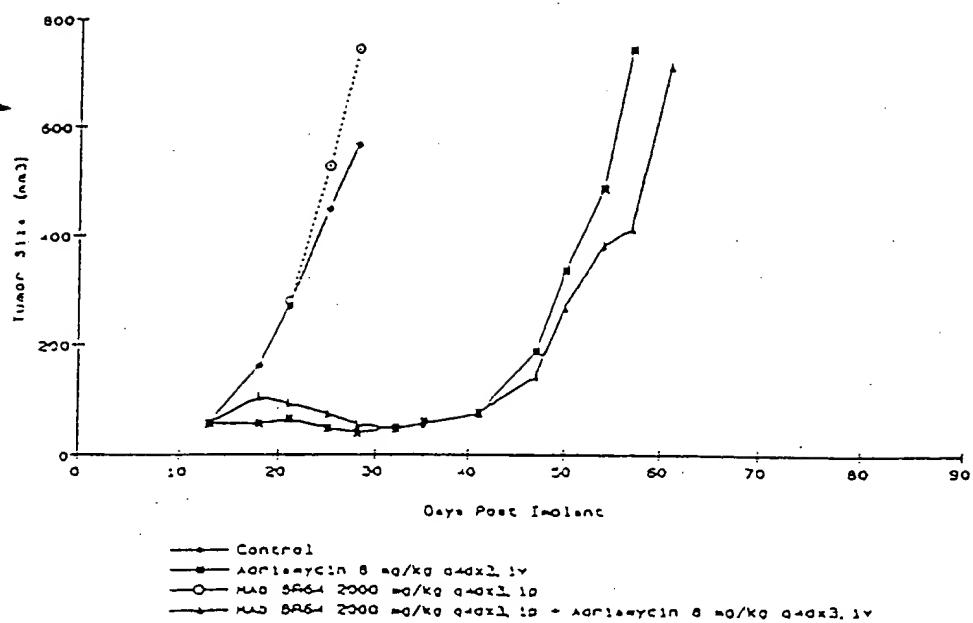


100

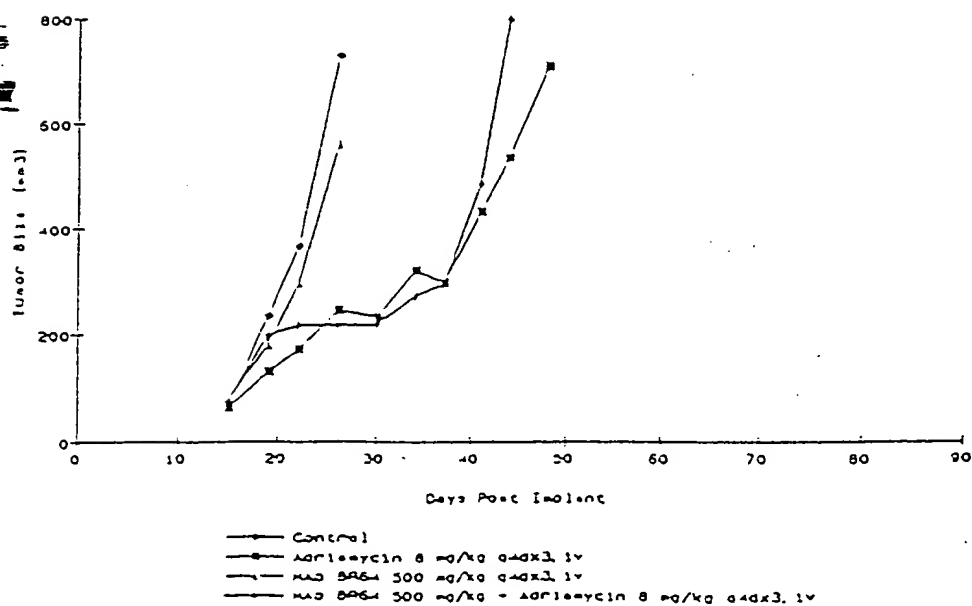


FIGURE 53 a/b

(a)



(b)



Days Post Inoculation	Tumor Size (mm) - Circles	Tumor Size (mm) - Squares	Tumor Size (mm) - Triangles
0	100	100	100
10	150	120	110
20	250	200	180
30	350	300	250
40	450	400	320
50	550	500	400
60	650	550	450
70	700	580	480
80	730	600	500
90	750	600	450

Year	1970	1971	1972	1973	1974	1975	1976	1977	1978	1979	1980	1981	1982	1983	1984	1985	1986	1987	1988	1989	1990	1991	1992	1993	1994	1995	1996	1997	1998	1999	2000	2001	2002	2003	2004	2005	2006	2007	2008	2009	2010	2011	2012	2013	2014	2015	2016	2017	2018	2019	2020	2021	2022	2023	2024	2025	2026	2027	2028	2029	2030	2031	2032	2033	2034	2035	2036	2037	2038	2039	2040	2041	2042	2043	2044	2045	2046	2047	2048	2049	2050	2051	2052	2053	2054	2055	2056	2057	2058	2059	2060	2061	2062	2063	2064	2065	2066	2067	2068	2069	2070	2071	2072	2073	2074	2075	2076	2077	2078	2079	2080	2081	2082	2083	2084	2085	2086	2087	2088	2089	2090	2091	2092	2093	2094	2095	2096	2097	2098	2099	2100
1970	1971	1972	1973	1974	1975	1976	1977	1978	1979	1980	1981	1982	1983	1984	1985	1986	1987	1988	1989	1990	1991	1992	1993	1994	1995	1996	1997	1998	1999	2000	2001	2002	2003	2004	2005	2006	2007	2008	2009	2010	2011	2012	2013	2014	2015	2016	2017	2018	2019	2020	2021	2022	2023	2024	2025	2026	2027	2028	2029	2030	2031	2032	2033	2034	2035	2036	2037	2038	2039	2040	2041	2042	2043	2044	2045	2046	2047	2048	2049	2050	2051	2052	2053	2054	2055	2056	2057	2058	2059	2060	2061	2062	2063	2064	2065	2066	2067	2068	2069	2070	2071	2072	2073	2074	2075	2076	2077	2078	2079	2080	2081	2082	2083	2084	2085	2086	2087	2088	2089	2090	2091	2092	2093	2094	2095	2096	2097	2098	2099	2100	

FIGURE 54

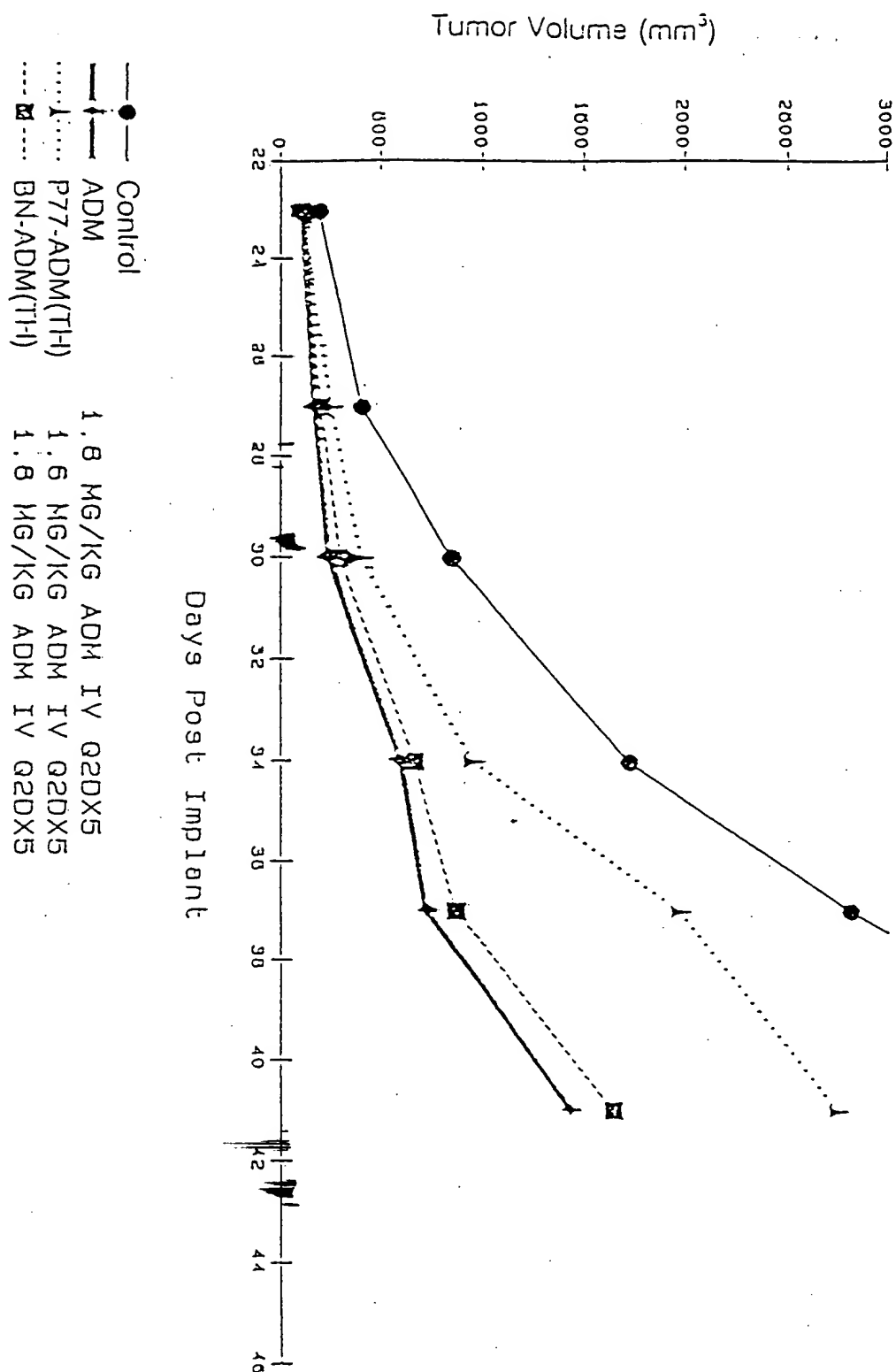


FIGURE 55

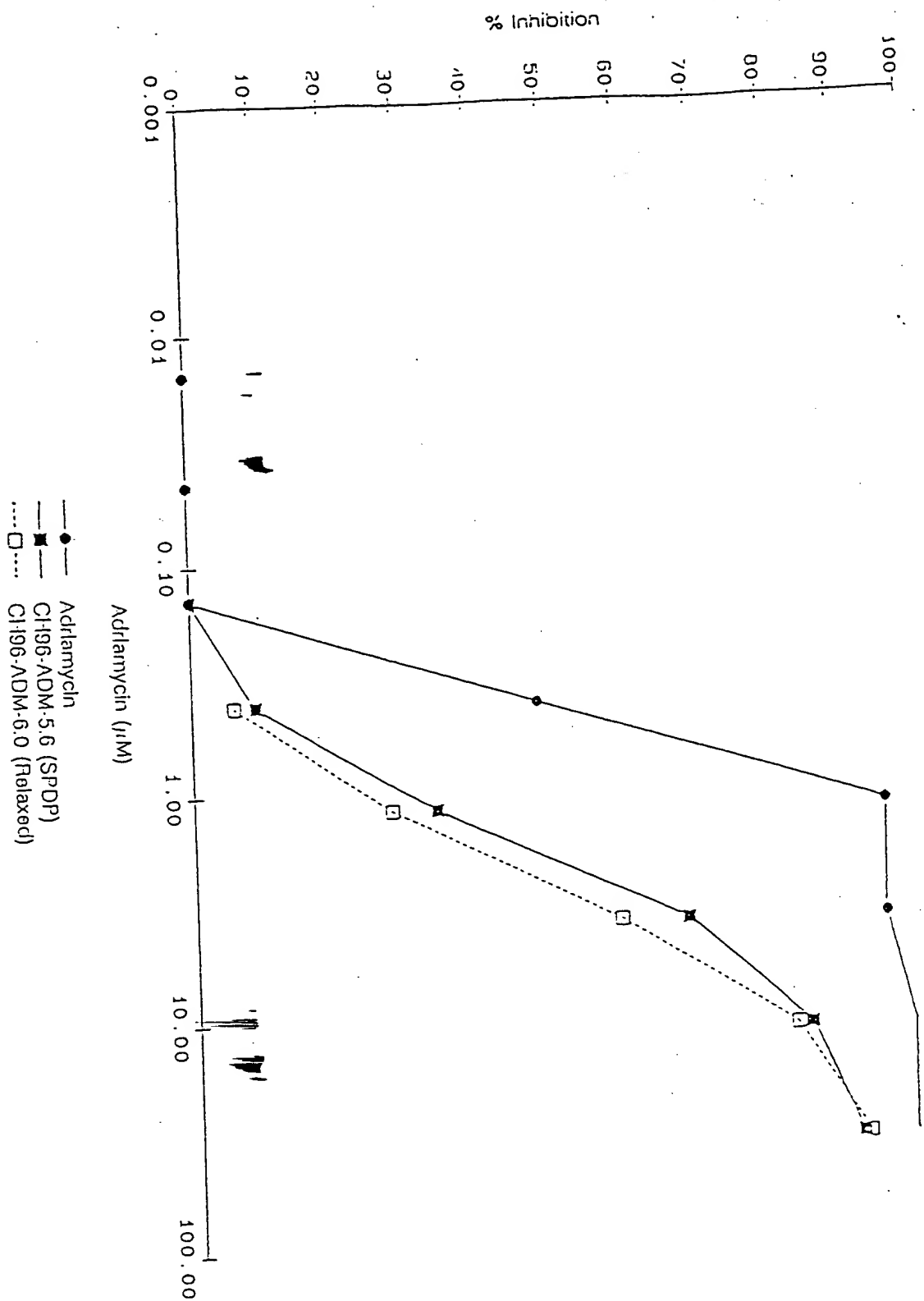


FIGURE 56

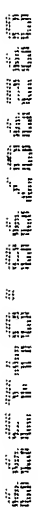


FIGURE 57

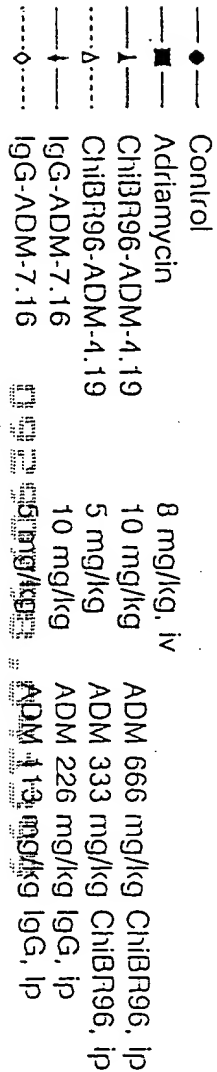


FIGURE 58

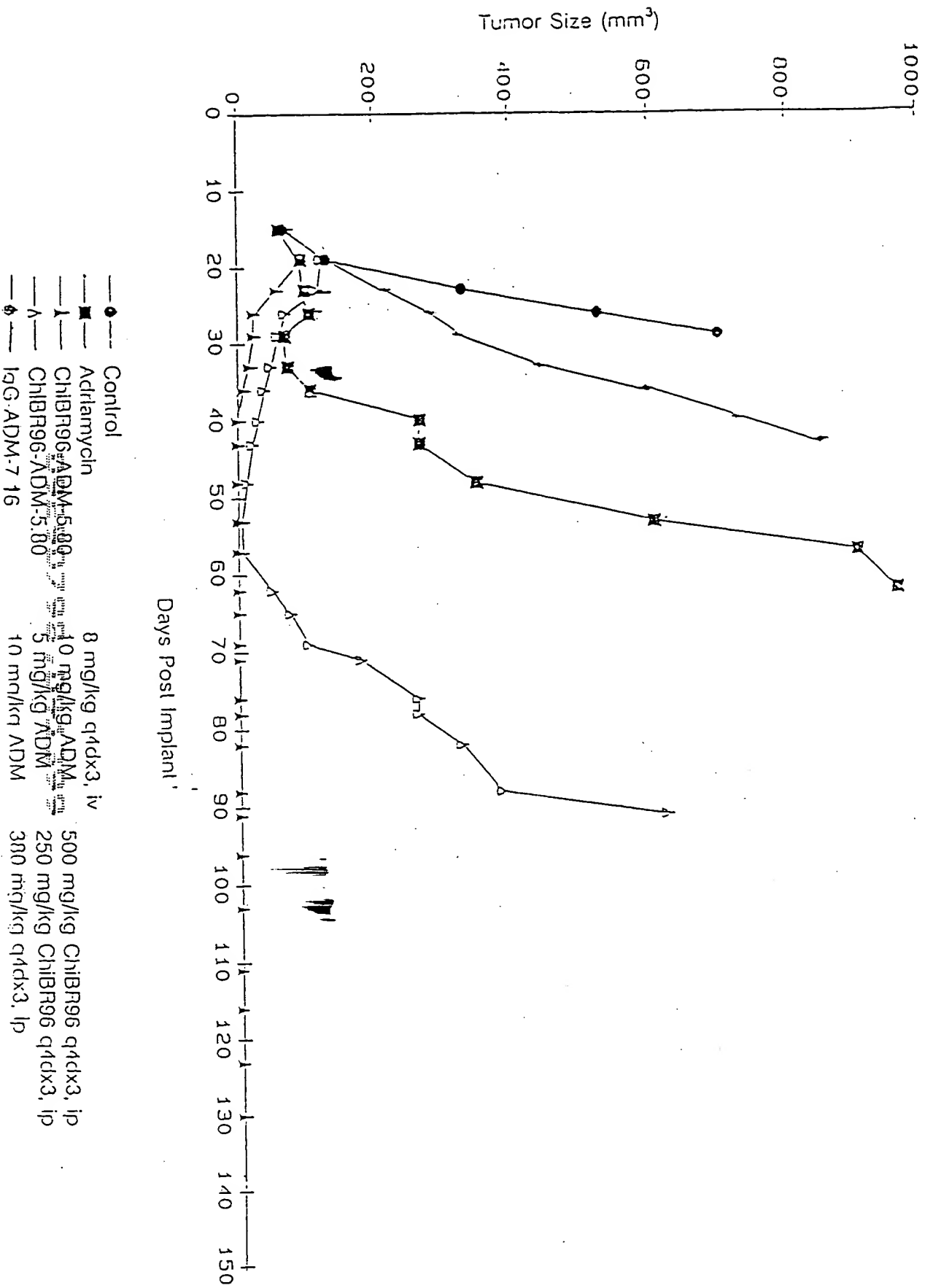


FIGURE 59

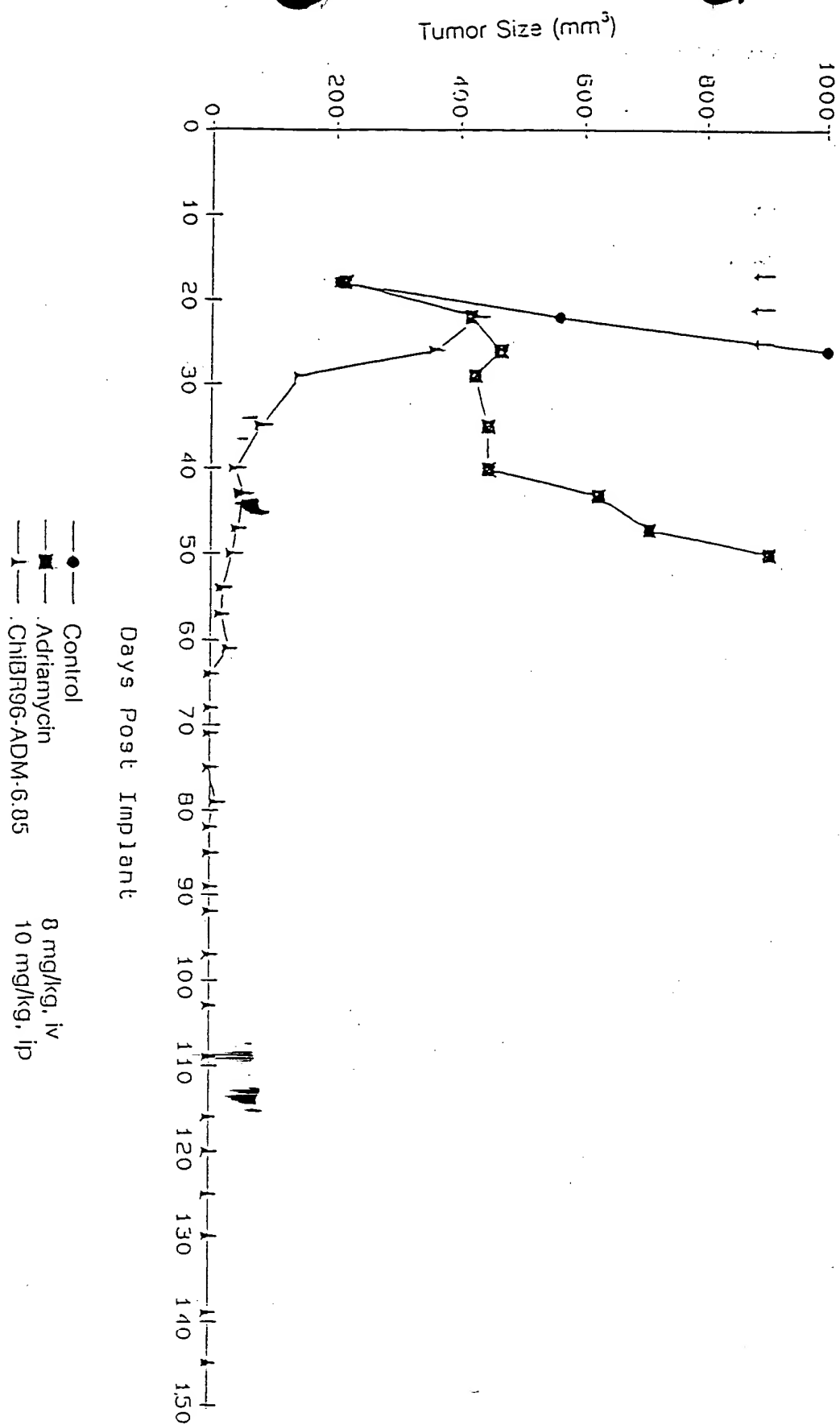


FIGURE 60

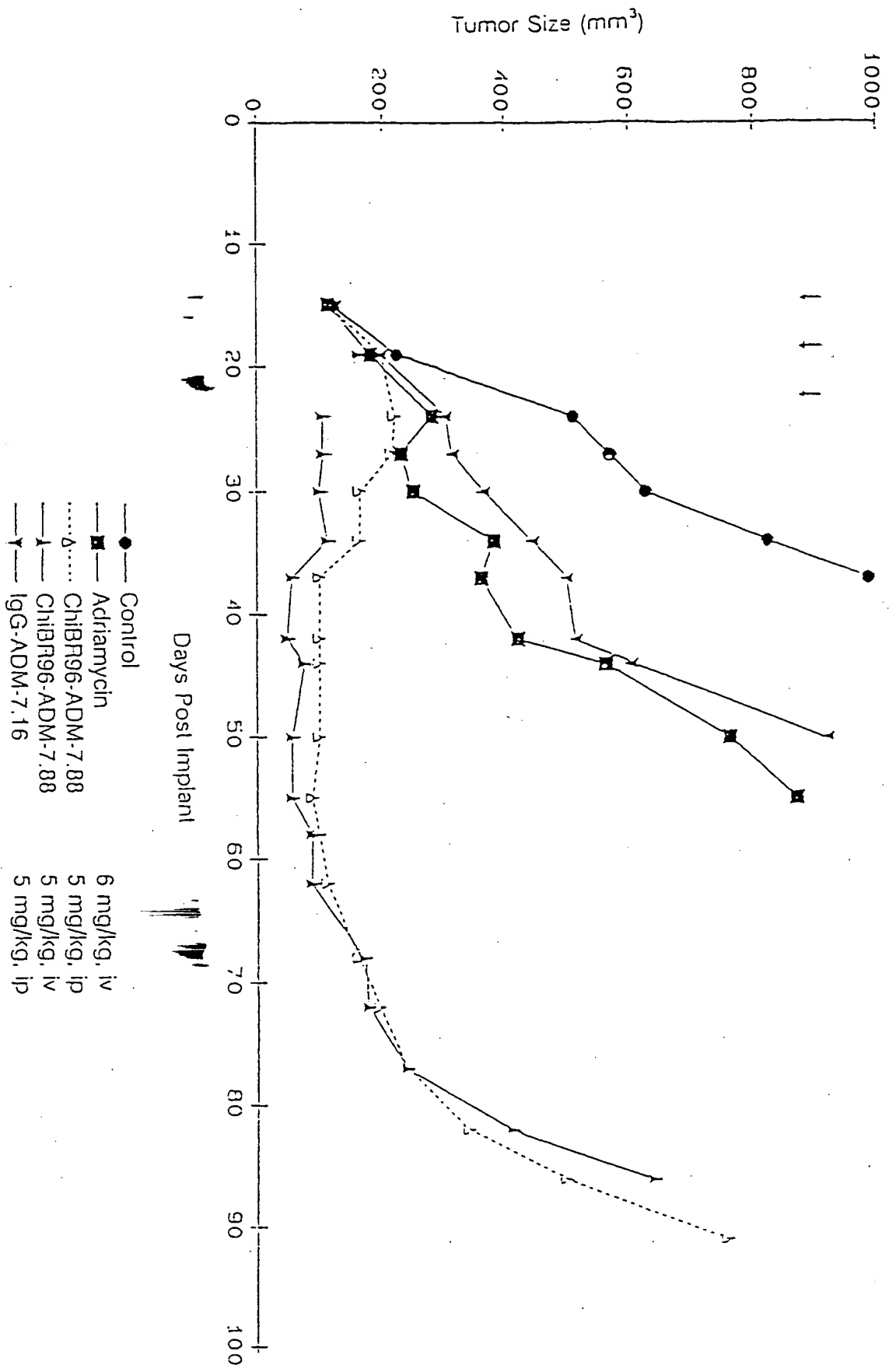


FIGURE 60

FIGURE 61

